OXFORD GENETICS

GENETICS, 2021, 217(2), iyab003
DOI: 10.1093/genetics/iyab003
Advance Access Publication Date: 13 January 2021
Fungal Genetics and Genomics

Comprehensive genetic analysis of adhesin proteins and their role in virulence of *Candida albicans*

Sierra Rosiana,[1] Liyang Zhang,[2] Grace H. Kim,[1] Alexey V. Revtovich,[2] Deeva Uthayakumar ,[1] Arjun Sukumaran,[1] Jennifer Geddes-McAlister,[1] Natalia V. Kirienko ,[2,*] and Rebecca S. Shapiro [1,*]

[1]Department of Molecular and Cellular Biology, University of Guelph, Guelph, ON NIG 2W1, Canada
[2]Department of BioSciences, Rice University, Houston, TX 77005, USA

*Corresponding authors: shapiror@uoguelph.ca (R.S.S); kirienko@rice.edu (N.V.K)

Abstract

Candida albicans is a microbial fungus that exists as a commensal member of the human microbiome and an opportunistic pathogen. Cell surface-associated adhesin proteins play a crucial role in *C. albicans'* ability to undergo cellular morphogenesis, develop robust biofilms, colonize, and cause infection in a host. However, a comprehensive analysis of the role and relationships between these adhesins has not been explored. We previously established a CRISPR-based platform for efficient generation of single- and double-gene deletions in *C. albicans*, which was used to construct a library of 144 mutants, comprising 12 unique adhesin genes deleted singly, and every possible combination of double deletions. Here, we exploit this adhesin mutant library to explore the role of adhesin proteins in *C. albicans* virulence. We perform a comprehensive, high-throughput screen of this library, using *Caenorhabditis elegans* as a simplified model host system, which identified mutants critical for virulence and significant genetic interactions. We perform follow-up analysis to assess the ability of high- and low-virulence strains to undergo cellular morphogenesis and form biofilms *in vitro*, as well as to colonize the *C. elegans* host. We further perform genetic interaction analysis to identify novel significant negative genetic interactions between adhesin mutants, whereby combinatorial perturbation of these genes significantly impairs virulence, more than expected based on virulence of the single mutant constituent strains. Together, this study yields important new insight into the role of adhesins, singly and in combinations, in mediating diverse facets of virulence of this critical fungal pathogen.

Keywords: fungal genetics; fungal pathogenesis; *Candida albicans*; *Caenorhabditis elegans*; host–pathogen interactions; genetic interaction analysis; adhesins

Introduction

Fungal pathogens have been emerging as a significant threat to human health, resulting in over 1.6 million deaths worldwide each year (Bongomin *et al.* 2017; Denning 2017; Geddes-McAlister and Shapiro 2019). Despite fungal pathogens affecting over 1 billion people each year, they still remain relatively understudied compared with many other infectious disease pathogens (Denning 2017; Fisher *et al.* 2020). *Candida albicans* is amongst the most pervasive fungal pathogens of humans, and can cause infectious disease ranging from acute mucosal infections, to systemic candidiasis with extremely high morbidity and mortality rates (Pfaller and Diekema 2007; Kullberg and Arendrup 2016; Bongomin *et al.* 2017). *Candida albicans* is an opportunistic pathogen present in the gastrointestinal tract, skin, reproductive tract, and oral cavity of most healthy adults. It asymptomatically colonizes many tissues of the human body, and may overgrow if there is a perturbation or depression of the host immune system, including treatment with antibiotics, organ transplants in combination with immunosuppressive drugs, or diseases such as HIV/AIDS (Kullberg and Arendrup 2016).

The success of *C. albicans* as a human pathogen relies on multiple virulence strategies, including morphological plasticity and robust biofilm formation (Shapiro *et al.* 2011; Sudbery 2011; Mayer *et al.* 2013). *C. albicans* is a polymorphic yeast, and its ability to reversibly transition between yeast and filamentous growth states (including hyphal and pseudohyphal growth) is a critical component of this pathogen's virulence (Sudbery 2011). *C. albicans* is capable of forming robust biofilms, not only on host tissues, but also on hospital equipment and medical implants such as catheters, pacemakers, and prosthetics (Finkel and Mitchell 2011; Nobile and Johnson 2015; Lohse *et al.* 2018). With the rising usage of medical implants, instances of implant-related infections are on the rise, with the majority of these infections associated with microbial biofilms (Finkel and Mitchell 2011; Nobile and Johnson 2015; Tsui *et al.* 2016; Lohse *et al.* 2018). As with many other microbial pathogens, *C. albicans* biofilms are typically resilient to many external stressors such as antifungals and host defense factors, making *C. albicans* significantly more difficult to treat in a biofilm state (Nobile and Johnson 2015; Tsui *et al.* 2016; Sharma *et al.* 2019).

Received: October 22, 2020. **Accepted:** December 31, 2020

Candida albicans pathogenesis is significantly impacted by its adherence abilities, and indeed the most frequently isolated pathogenic *Candida* species are those with the greatest adhesive capacities, and these tend to be more pathogenic than other strains (Calderone and Braun 1991; Hoyer 2001). While many factors are involved in *C. albicans* adhesion, it is known that this process is largely due to the expression of fungal cell wall proteins, including adhesins, which are highly expressed on filamentous cells, and involved in surface adhesion, biofilm formation, and host colonization (Sundstrom 1999; de Groot *et al.* 2013; Lipke 2018). A family of adhesin proteins of particular interest in *C. albicans* is the *ALS* (agglutinin-like sequence) family of cell surface glycoproteins (Hoyer 2001). This family shares a four domain structure consisting of a high-complexity N-terminal domain that mediates protein-ligand interactions with host cells or other substrates, a threonine-rich domain, a low-complexity central domain that is highly variable in length, and a C-terminal domain that anchors the adhesin to the fungal cell wall via a glycosylphosphatidylinositol (GPI) anchor (Hoyer 2001; Hoyer and Cota 2016). There are eight *ALS* loci currently described in *C. albicans*: *ALS1-7* and *ALS9* (Hoyer *et al.* 2008; Hoyer and Cota 2016). Other families of adhesins have also been identified, including *HWP*, *IFF*, and *HYR* (de Groot *et al.* 2013). Some *C. albicans* adhesins, such as *ALS1* and *ALS3*, have been subject to fairly comprehensive molecular genetic and biochemical analysis, and have well-described roles in various aspects of adhesion, host–pathogen interactions, filamentation, and fungal virulence (Fu *et al.* 1998, 2002; Hoyer *et al.* 1998; Sheppard *et al.* 2004; Zhao *et al.* 2004; Ibrahim *et al.* 2005; Phan *et al.* 2007; Almeida *et al.* 2008; Nobile *et al.* 2008; Cleary *et al.* 2011; Donohue *et al.* 2011a), while other adhesins remain incompletely described or fully uncharacterized. Additional evidence indicates that the numerous *C. albicans* adhesins have complex interactions and may have complementary, compensatory, or redundant functions (Zhao *et al.* 2004, 2005; Nobile *et al.* 2008; Shapiro *et al.* 2018a).

Given the complex interplay between *C. albicans* adhesin proteins, a useful strategy to assess the function of these factors is through genetic interaction analysis. Genetic interaction analysis is a powerful strategy that typically takes advantage of single- and double-gene deletion strains to assess epistatic interactions between genes, and can be used to organize gene products into pathways, identify genetic synergies and redundancies, and predict gene function (Dixon *et al.* 2009; Baryshnikova *et al.* 2013). While genetic interaction analysis has been exploited widely in model organisms (Butland *et al.* 2008; Costanzo *et al.* 2010, 2016; Babu *et al.* 2011; Norris *et al.* 2017), it has more recently been employed as a tool to dissect genetic interaction networks in diverse microbial pathogens, including *C. albicans* (Glazier *et al.* 2017, 2018; Shapiro *et al.* 2018a, 2018b; Glazier and Krysan 2020; Halder *et al.* 2020). Our previous work established a CRISPR-Cas9-based gene drive array (GDA) platform, which permits facile, precise and efficient creation of combination gene knockouts in *C. albicans*, which we applied to construct a library of 144 mutants, comprising 12 unique adhesin genes deleted singly, and in every possible combination of double deletions (Shapiro *et al.* 2018a; Halder *et al.* 2019). This library enables the analysis of complex genetic interactions between adhesins and their prospective roles in *C. albicans*' adhesion; it further enables the identification of combinations of genes which, when deleted together, may interfere with fungal biofilm formation, host–pathogen interactions, or virulence.

Studying putative *C. albicans* virulence factors, such as adhesins, requires the use of a model host to assess fungal pathogenicity *in vivo*. *Caenorhabditis elegans* is a free-living nematode that has been exploited as a simple and practical model for studying host–pathogen interactions with diverse microbial pathogens (Aballay and Ausubel 2002; Marsh and May 2012; Issi *et al.* 2017; Kumar *et al.* 2020), including *C. albicans* (Pukkila-Worley *et al.* 2009, 2011; Jain *et al.* 2013; Elkabti *et al.* 2018; Feistel *et al.* 2019) and other fungal pathogens (Mylonakis *et al.* 2002b; Tang *et al.* 2005; Huang *et al.* 2014; Ahamefule *et al.* 2020; Hernando-Ortiz *et al.* 2020). One of the first papers to utilize *C. elegans* as a host for *C. albicans* elegantly demonstrated that virulence in *C. elegans* utilized some of the same processes that are used in mammalian hosts, such as biofilm and hyphal formation (Breger *et al.* 2007). The use of *C. elegans* to study *C. albicans* virulence has been recently reviewed in detail (Elkabti *et al.* 2018).

Caenorhabditis elegans is a simple and cost-effective model organism that is readily propagated and stored, and lends itself to high-throughput screening of microbial pathogens (Moy *et al.* 2009; Kirienko *et al.* 2013, 2016). *C. elegans* host–pathogen interactions have many conserved features that are shared with mammalian species, making it an advantageous model for studying human disease and infections. The intestinal epithelial cells of *C. elegans* have morphological features, such as microvilli, that are similar to mammalian epithelial cells, and it is estimated that 40%–60% of genes in *C. elegans* have human orthologs (*C. elegans* Sequencing Consortium 1998; McGhee 2007; Kumar *et al.* 2020). With regards to *C. albicans* infection, many biological mechanisms by which *C. albicans* infects *C. elegans* are similar in humans and nematodes, and *C. elegans* host immune responses to pathogens are remarkably conserved (Gravato-Nobre and Hodgkin 2005; Kim and Ausubel 2005; Pukkila-Worley and Mylonakis 2010). Once ingested by *C. elegans*, *C. albicans* can cause a persistent lethal infection, making monitoring the infection relatively simple for research purposes (Pukkila-Worley and Mylonakis 2010; Elkabti *et al.* 2018). Many *C. albicans* genes that are known to be required for murine infection are similarly required for infection in *C. elegans* (Pukkila-Worley *et al.* 2009; Elkabti *et al.* 2018).

C. elegans' utility as a model organism in the study of innate immunity, while powerful, does require certain caveats. For example, this nematode lacks several important signaling pathways that are involved for cell-mediated immunity, including the MyD88 adaptor, the NF-κB transcription factor, and the immune function associated with its sole Toll-like receptor, TOL-1, remains limited (Irazoqui *et al.* 2010; Ermolaeva and Schumacher 2014). It is also important to note that the system lacks both adaptive immunity and professional immune cells. Despite these limitations, this model has demonstrated remarkable versatility and usefulness for innate immune studies ranging from the identification of the pervasive interplay between canonical stress responses and innate immunity, the connections between innate immunity and the nervous system, and between pro-immune and pro-longevity pathways. It is also a versatile platform for high-throughput and high-content screening.

Here, we perform systematic characterization and genetic interaction analysis of a *C. albicans* library of adhesin (or adhesin-like) gene mutants (de Groot *et al.* 2013), deleted for these factors singly or in combinations of double knockouts. We use *C. elegans* as a model host system to perform screening of our *C. albicans* library of 144 adhesin mutant strains, and identify single and combination genetic mutations that significantly alter fungal virulence. Following up on the strains with the highest and lowest levels of virulence, we characterize phenotypes associated with other virulence traits, including host colonization, biofilm formation, and cellular morphogenesis. We find that many

virulence-associated phenotypes are uncoupled under our experimental conditions. We further perform genetic interaction analysis to identify and characterize significant negative genetic interactions, whereby double mutants are significantly impaired in virulence based on what we would predict given the virulence of their single mutant counterparts. Together, this study comprehensively characterizes the roles of single- and double-adhesin mutant strains in fungal pathogenicity, with important implications for understanding fungal virulence and host interactions.

Materials and methods

Caenorhabditis elegans–*C. albicans* liquid infection assay and screening

The *C. elegans*–*C. albicans* infection assay was performed with slight modifications to the previous method (Breger *et al.* 2007). In brief, *C. elegans glp-4(bn2)* mutants were reared on NGM media seeded with concentrated *E. coli* OP50 media until they reached the young adult stage (1 day at room temperature and then shifted to 25°C for 2 days) (Kirienko *et al.*, 2014).

C. albicans strains were cultured overnight in 96-well deep-well plates containing 300 μL YPD and incubated at 37°C. OD_{600} of each plate was read and cultures were diluted with S Basal to normalize *C. albicans* density. 384-well assay plates were set, with final media composition of 10% BHI, *C. albicans* at $OD_{600} = 0.03$, 3.5 μg/mL cholesterol, and S Basal (to bring the final volume to 50 μl/well). Using a COPAS FlowPilot (a large-bore fluorescence-activated worm sorter, analogous to a FACS machine), and LP (large particle) Sampler (Union Biometrica, MA), 25 *C. elegans* nematode worms were added to each well. Plates were covered with breathable membranes and incubated for 72 h at 25°C. OD_{600} was read for each plate. Plates were washed 5 times with S Basal, then liquid was aspirated using an EL 406 Plate washer/Liquid dispenser (BioTek, VT). Fifty microliters of 0.01% tween in S Basal were added to each well to limit worms adhering to pipette tips; worms were then transferred to new 384-well plates to minimize background. Plates were washed 5 times with S Basal to remove transferred pathogens, and then liquid was aspirated. Fifty microliters of SytoxOrange stain (0.2 μL Sytox/1 mL S Basal) were loaded into each well. Plates were incubated 12–16 h in a dark place at room temperature. Plates were washed 5 times with S Basal. Plates were imaged with both bright field and red channel RFP using a Cytation 5 multimode plate reader/imager (BioTek, VT). Images were analyzed for worm survival using CellProfiler, as previously described (Anderson *et al.* 2018). Statistical analysis was performed on all data to ensure significance. *Caenorhabditis elegans* liquid infection assay data were initially checked using the coefficient of variation (CV) and outliers were removed to obtain CV scores of 0.5 or less in as many strains as possible. The remaining strains had CV scores of less than 1. The selected mutants in all datasets were subjected to one-way ANOVA tests to compare each strain to the wild type.

Genetic interaction analysis

Each single mutant tested in this research was assigned a virulence score based on the results of the *C. elegans* infection assay. The virulence score of the wild type was normalized to 1, and the results from all other strains were divided by the wild-type results to achieve these relative virulence scores. The virulence scores of each single parent strain were multiplied by one another and the product became the predicted virulence score of the double mutants. Genetic interaction analysis was based on deviation from predicted virulence scores. If the double mutant's actual score was significantly different from its predicted score, it was considered a "hit." Genetic interaction analysis was done using R. First, the program bound all the replicate results together, labeled each single mutant and created a single dataset with the library's unique combinations. A two-sided *t*-test was used to compare the predicted and actual virulence scores. A positive interaction had an adjusted p-value < 0.05 and a deviation that is greater than the predicted score. A negative interaction had an adjusted p-value < 0.05 and a deviation that is lower than the predicted score. The R program used for this GI analysis can be found here: https://github.com/kieran11/wormdata

Colonization assay

To assess *C. elegans* colonization by *C. albicans* following agar- or liquid-based infection, worms were infected as described above. After 24 h, worms were transferred onto a clean plate and allowed to crawl away from *C. albicans*. Then they were transferred via pick to a 1.5 mL microcentrifuge tube containing S Basal with 1% levamisole, and incubated 10 min until all worms were paralyzed. Worms were washed 5–6 times in S Basal containing 0.01% Triton X-100 to remove residual fungi. After the final wash, worms were resuspended in 200 μL of 0.1% Triton-X 100 in S Basal and vortexed for 1 min using zirconium beads (Thermofisher Scientific, NC0442292). The resulting lysate was serially diluted five-fold and plated onto YPD agar plate to quantify the number of colony forming units (CFU) per unit volume. This value was then used to derive the average number of CFUs per worm in each sample. The assay was performed using three biological replicates, each of them consisting of three technical replicates, with 15 worms per technical replicate. Colonization, rather than cuticle attachment, of the fungus was verified using a strain of *C. albicans* that expressed GFP. As expected, the CFUs identified were from inside of the host; no apparent fungus was seen on the surface.

Caenorhabditis elegans–*C. albicans* agar-based killing assay

Kim et al. (2020) recently outlined an agar killing assay as a nematode infection model to study fungal pathogenesis. Briefly, *C. elegans glp-4* eggs were extracted with worm bleach and resuspended in S Basal to establish a fresh stock of worms. The *C. elegans* worms were then counted on an NGM plate under a stereomicroscope and 5000–6000 worms dropped onto two superfood agar plates, which were left overnight at room temperature then moved to 25°C for an additional two nights. *C. albicans* strains were incubated overnight in 1 mL of YPD at 37°C and 250 rpm and then 70 μL of culture was spread onto a BHI-kanamycin (Kan) plate, which were then incubated for 16 h at 30°C. Approximately 6 mL of S Basal was dispensed onto each *C. elegans* superfood agar plate to dislodge the worms. The worms were then washed 3 times with S Basal before being made into a solution of 2 worms per μL of S Basal. 45–55 worms were transferred onto each *C. albicans*-inoculated BHI-Kan plate, which were then left at room temperature for 1 h before being stored overnight at 25°C. Dead worms were counted and removed with a platinum wire worm pick from the plates under a stereomicroscope daily until all worms were dead.

Quantitative, real-time reverse-transcription PCR

For quantitative, real-time reverse-transcription PCR (qPCR), *C. albicans* were prepared as for agar- or liquid-based assays. Next, *C. albicans* was either scraped off the plate and resuspended in S Basal or centrifuged down (for agar or liquid assays, respectively).

RNA was extracted from a ~100 μL fungal pellet. RNA was purified by vortexing the fungal sample with glass beads and then subsequent Trizol extraction with BCP as a phase-separating agent, as previously described (Kirienko *et al.* 2019). Reverse transcription was performed using an AzuraQuant cDNA Synthesis Kit (Azura). qPCR was conducted in a CFX-96 real-time thermocycler (Bio-Rad) using SYBR green AzuraQuant Fast Green Fastmix (Azura). Fold-changes were calculated using a ΔCt method with actin as a housekeeping gene. Cycling parameters and primer sequences are available upon request. For each experiment, at least three biological replicates were performed.

Filamentation assay and analysis

C. albicans strains were incubated overnight in 5 mL YPD at 37°C and 250 rpm. OD_{600} of each culture was taken. Cultures were diluted with fresh YPD media to normalize to the same OD_{600} value. *C. albicans* was subcultured into 5 mL YPD with 10% fetal bovine serum (FBS). Subcultures were incubated at 37°C and 350 rpm for 4 h. Ten microliters of each culture were pipetted onto a microscope slide and visualized under phase microscopy at 40X magnification using a Leica DM 2000 LED microscope. Images of each strain were taken with a Leica ICC50 W camera. Images were analyzed using the ImageJ program and MicrobeJ plugin. Analysis involved using ImageJ to count the number of yeast cells and filamentous cells in each image as well as measure the length of each filamentous cell in each image.

Biofilm assay

Candida albicans strains were incubated overnight in 5 mL YPD at 37°C and 250 rpm. OD_{600} of each culture was taken. Cultures were diluted with BHI+Kan media to normalize to the same OD_{600} value. Strains were subcultured into flat-bottomed 96-well polystyrene plates containing 100 μL of BHI+Kan and 100 μL of culture per well. Two hundred microliters of YPD per well in one row served as a negative control. 96-well plates were wrapped in tinfoil and incubated at 37°C for 72 h. One hundred and twenty microliters of planktonic cells from each well were transferred to new 96-well plates, then read in a plate reader at OD_{600}. Plates were washed twice with 200 μL PBS and left upside down to dry in a fume hood. One hour later or once dry, 90 μL of XTT (1 mg/mL PBS) and 10 μL of PMS (0.32 mg/mL H_2O) was added to each well. Plates were wrapped in tinfoil and incubated for 2 h at 30°C. Plates were read at 490 nm using a Tecan infinite M nano spectrophotometer. The XTT biofilm growth values were normalized to planktonic cell growth.

Data and reagent availability

Candida albicans–C. elegans virulence screening data are available in Supplementary Table S1. The R program used for this GI analysis can be found here: https://github.com/kieran11/wormdata. All *C. albicans* strains used as part of this research will be made available upon request. Supplemental Material available at figshare: https://doi.org/10.25386/genetics.13517432.

Results

Caenorhabditis elegans infection assay identifies avirulent *C. albicans* adhesin mutants

First, we aimed to assess the virulence profiles of a library of *C. albicans* adhesin single- and double-gene deletion mutants (Shapiro *et al.* 2018a), to assess the role of these factors, singly or in combination, in fungal pathogenicity. This adhesin mutant library consisted of 144 adhesin mutants, representing 12 single adhesin gene deletions, and 66 double adhesin gene deletions with "reciprocal pairs," where a reciprocal pair refers to the same mutant genotype, but generated by mating opposite mating type haploids (*i.e.* *a*Δ/*b*Δ and *b*Δ/*a*Δ). In order to assess virulence, we used a high-throughput screening model with *C. elegans* as a model host. Young adult *C. elegans* worms were added to 384-well plates containing each of the *C. albicans* mutant strains, and incubated for 72 h. After infection, plates were washed to remove *C. albicans* and dead *C. elegans* were stained with a cell-impermeant fluorescent dye (Figure 1A and see Materials and Methods for additional details). This infection assay was repeated in six replicates. Increased survival of the *C. elegans* host indicated less virulence by the particular mutant strain of *C. albicans*. Figure 1B depicts an example of bright field imaging that allows visualization of all worms after infection. Figure 1C depicts examples of fluorescent images, where only dead *C. elegans* worms are stained and are visible with fluorescence. Worm death is monitored and calculated based on the ratio of the area of fluorescence to the area of total worms in brightfield.

The wild-type strain, with no gene deletions, was used to determine baseline virulence, and was compared with the 144 mutant strains for ability to cause death in the *C. elegans* host. As predicted, the wild-type strain showed a high level of virulence toward *C. elegans* with greater than 50% of worms killed during the course of the infection assay (Figure 2, Supplementary Table S1). Overall, many of the adhesin mutants were found to be impaired in virulence, compared with the wild-type strain (Figure 2): 24 out of 78 unique genotypes (12 single mutants and 66 double mutant genotypes) led to significant reduction in worm death compared to the wild-type strain ($P < 0.05$, ANOVA, Supplementary Table S1). Interestingly, there was no positive correlation between growth rates and virulence. In contrast, a weak negative correlation was observed, suggesting that strains with lower virulence grew to a higher optical density (Supplementary Figure S1).

Of the mutants with significantly impaired virulence, 22 were double mutants, and two (*als1*Δ and *als5*Δ) were single mutants. Mutation of *als1*Δ, and to a lesser extent *als5*Δ, singly or in combination with other genes, attenuated the ability of the pathogen to kill the host to the greatest extent, suggesting that these adhesin genes significantly contribute to *C. albicans*' virulence in this *C. elegans* infection model. This is in line with previous studies in mammalian models that have demonstrated a key role for *ALS1* as an important virulence regulator (Braun *et al.* 2000; Kamai *et al.* 2002; Alberti-Segui *et al.* 2004; Zhao *et al.* 2004).

The five most virulent strains (excluding wild-type) were *als3*Δ*iff4*Δ, *als9*Δ*iff4*Δ, *hwp2*Δ, *als3*Δ*hwp2*Δ, and *als9*Δ*eap1*Δ; all of which displayed similar death percentages to the wild-type strain (>50% of worms dead). The single mutant counterpart strains of these mutants, *hwp2*Δ, *als3*Δ, *iff4*Δ, *als9*Δ, and *eap1*Δ all show comparatively high virulence, indicating that these adhesins are not essential for virulence, at least in this infection model. The least virulent strains were *hyr1*Δ*als1*Δ, *als7*Δ*als5*Δ, *als1*Δ*iff4*Δ, and *rbr1*Δ*als1*Δ. The three most significantly attenuated strains (*hyr1*Δ*als1*Δ, *als7*Δ*als5*Δ, and *als1*Δ*iff4*Δ, < 10% death) were selected for follow-up study. The single mutant strains, in order from least virulent to most virulent were as follows: *als1*Δ, *als5*Δ, *rbt1*Δ, *als9*Δ, *eap1*Δ, *rbr1*Δ, *hyr1*Δ, *als7*Δ, *hwp1*Δ, *iff4*Δ, *als3*Δ, and *hwp2*Δ. Several of these single adhesin factors with important roles in virulence in our *C. elegans* model (such as *als1*Δ and *rbt1*Δ), have been well-established as virulence regulators based on animal model studies (Braun *et al.* 2000; Kamai *et al.* 2002; Alberti-Segui *et al.* 2004; Zhao *et al.* 2004).

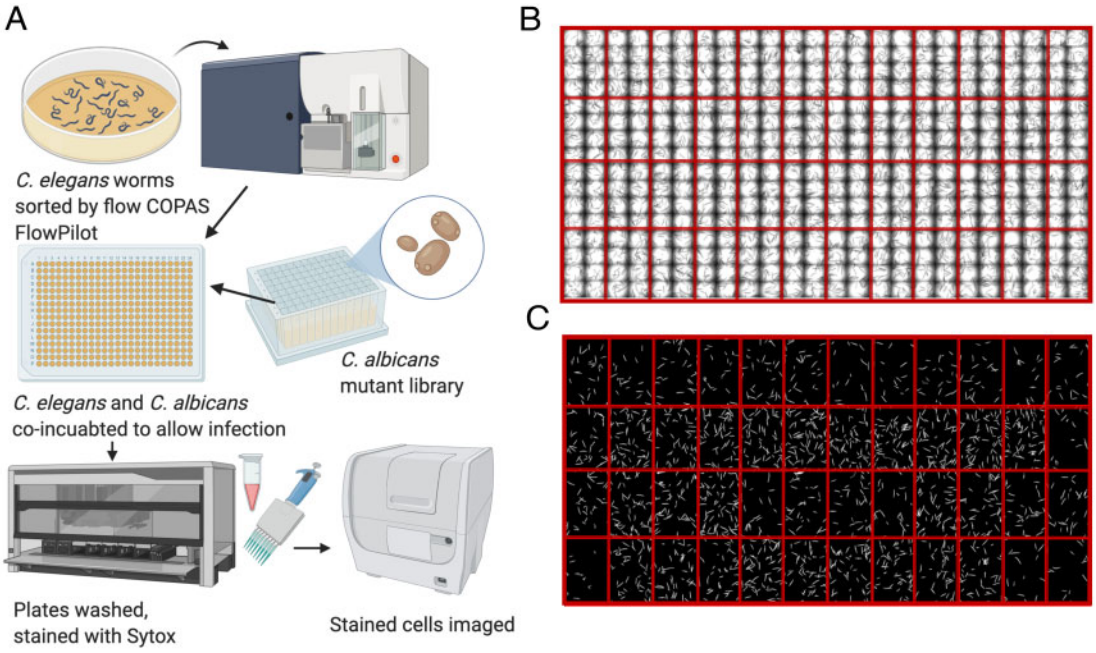

Figure 1 A protocol of *C. albicans*—*C. elegans* high-throughput screening for fungal virulence regulars. *C. elegans* is a model host for *C. albicans* fungal infection and can be used in high-throughput screening settings to identify regulators of fungal virulence. (A) A schematic indicating the workflow for the *C. albicans*—*C. elegans* infection assay. Worms were sorted by COPAS FP worm sorter and an equal number of worms were deposited into each well of a 384-well plate. *C. albicans* mutant strains (the single- and double-gene deletion library) were inoculated into the 384-well plate, and *C. albicans* and *C. elegans* were co-incubated to allow for infection. To stop the infection progression, plates were washed with a plate washer to remove *C. albicans*, and *C. elegans* were stained with a cell impermeant dye Sytox Orange to identify dead worms. Plates were then imaged in brightfield and fluorescence channels, and processed using Cell Profiler software to identify the total area of worms, as well as the area of fluorescence inside of the worms per each well. This figure was created using BioRender (biorender.com) (B) An example of brightfield imaging, which allows visualization of all of the worms (alive and dead) after infection. Red lines have been added to the image to depict the delineation between wells with the same strain of *C. albicans* inoculated. (C) Example of fluorescence microscopy images used to identify dead fluorescent worms stained with the cell-impermeant fluorescent dye, Sytox Orange. Only dead *C. elegans* worms were stained and visible with fluorescence. Red lines have been added to the image to depict the delineation between wells with the same strain of *C. albicans* inoculated (technical replicates).

The double mutant "reciprocal pairs" were all validated to ensure they indicate the same results. For example, *als1Δals3Δ* and *als3Δals1Δ* should theoretically show the same results because the same two genes were deleted, though the strains were generated independently. The majority of the mutants showed very similar data results between the reciprocal pairs, similar to what had been seen in previous analysis of this library (Shapiro *et al.* 2018a). Amongst the 66 total double deletion genotypes, 13 (*hwp1Δhwp2Δ*, *hwp1Δhyr1*, *als3Δhwp1Δ*, *als3Δhwp2Δ*, *als3Δiff4Δ*, *als5Δals9Δ*, *als5Δhwp1Δ*, *als5Δrbt1Δ*, *als7Δhwp1Δ*, *als7Δrbr1Δ*, *als9Δiff4Δ*, *als9Δrbr1Δ*, and *eap1Δhyr1Δ*) had a virulence difference between their reciprocal pairs of 10% points or more (*i.e.* if *aΔbΔ* resulted in 45% dead worms and *bΔaΔ* resulted in 55% dead worms). Differences between reciprocal pairs could be stochastic and associated with variation observed in the *C. elegans* virulence assays, or could be due to factors, including secondary mutations acquired through the transformation and/or mating process, or from off-target effects of CRISPR-Cas9.

Low- and high-virulence *C. albicans* mutants exhibit different ability to colonize *C. elegans*

Next, we examined the relationship between *C. albicans* colonization of *C. elegans* and strain virulence. As previously described, we focused on our assembled panel of six mutant strains, three with low virulence (*als1Δiff4*, *hyr1Δals5Δ*, *als7Δals5Δ*) and three with high virulence (*als3Δhwp2Δ*, *als3Δiff4Δ*, *als9Δiff4Δ*) (Figure 3A; $p < 0.0001$ pooled low- and high-virulence groups, Student's *t*-test). Sterile, young adult *glp-4(bn2)* worms were exposed to each *C. albicans* strain in a liquid pathogenesis assay for 24 h. Worms were then collected, washed, and lysed. Serially diluted fungi were plated on YPD agar media and colony-forming units were counted to establish the colonization potential of these different fungal mutants. Interestingly, significant differences were observed between the levels of colonization of low-virulence compared with high-virulence subsets (Figure 3B; $p < 0.05$ pooled low- and high-virulence groups, Student's *t*-test). Strains with lower virulence in the *C. elegans* infection assay, demonstrated increased capacity for worm colonization (Figure 3B). Interestingly, this contrasts with previous observations of bacterial pathogens that colonize *C. elegans*; in those cases, colonization and virulence directly (rather than inversely) correlated (Garsin *et al.* 2003; Evans *et al.* 2008; Kirienko *et al.* 2013). One possible explanation for this difference is that *C. elegans* detects pathogenic determinants or damage afflicted by the fungus during infection and responds with increased innate immune activity that restricts fungal colonization. This suggests an interesting trend amongst these fungal mutant strains that unlinks pathogen colonization potential and virulence.

Candida virulence mechanisms differ between liquid- and agar-based assays

Research using *C. elegans*-based pathogenesis models have convincingly demonstrated that the microbial virulence determinants are strongly influenced by the context of the infection assay (*e.g.* media composition, state of matter, etc.). For example, at least five distinct *C. elegans*–*Pseudomonas aeruginosa*

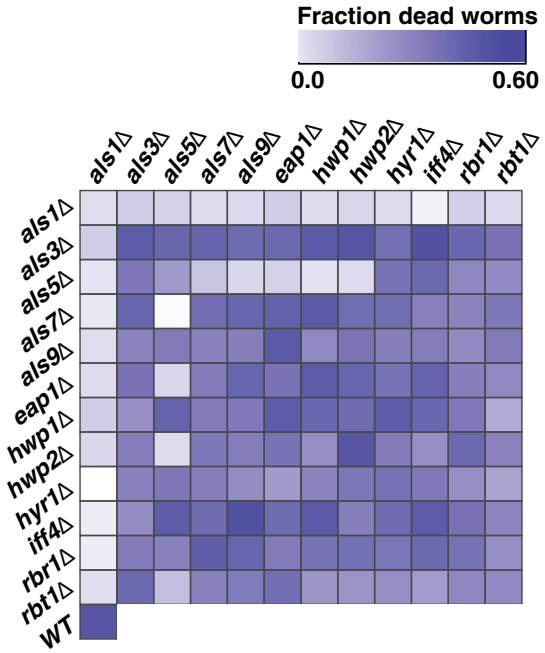

Figure 2 Multiple *C. albicans* adhesin mutant strains are impaired in virulence in *C. elegans* model of infection. When screened for virulence using *C. elegans* as a model host, *C. albicans* adhesin mutant strains displayed variable levels of virulence. The library of 144 single- and double-genetic mutant strains was screened for virulence, and the fraction of dead worms was established for each mutant strain. The heat map depicts the compiled and processed results from the experiment, with darker blue/purple squares indicating more worm death (higher fraction of dead worms), and white or lighter-colored squares indicating less death (lower fraction of dead worms). The heatmap shows virulence for each strain, averaged over at least four biological replicates. The heat map was generated using Morpheus matrix visualization and analysis software from the Broad Institute (https://software.broadinstitute.org/morpheus).

pathogenesis models have been described (Mahajan-Miklos *et al.* 1999; Tan *et al.* 1999; Gallagher and Manoil 2001; Zaborin *et al.* 2009; Kirienko *et al.* 2013; Utari and Quax 2013). To investigate whether this phenomenon holds true for *C. albicans*, host killing in an agar-based infection model was compared to data from the liquid-based *C. elegans* infection model. In this agar-based assay, *C. elegans* survival was scored daily until all the worms were dead. For a more direct comparison with the liquid-based assay, we extracted survival data for day 4. At this time, wild-type *C. albicans* has killed approximately 50% of worms, a value consistent with our observations from liquid-based assays. Interestingly, when pooled data for low- and high-virulence mutants were compared, we saw the reverse of the outcome from the liquid-based assay: strains that were highly pathogenic in liquid killing and had low colonization, also had low pathogenesis on solid media (Figure 3C; $p < 0.001$ pooled low- and high-virulence groups, Student's *t*-test). Kaplan–Mayer curves demonstrating longitudinal survival are shown in Supplementary Figure S2.

We hypothesized that the relative expression of adhesin genes, and perhaps the compensatory upregulation of different adhesin genes in different mutant strain backgrounds under variable growth conditions, may underlie these differences. Such compensatory upregulation of adhesins has been predicted to be involved with other fungal adhesins, and may explain why deletion of adhesins *ALS5*, *ALS6*, and *ALS7* in *C. albicans* leads to increased adhesion to human vascular endothelial cells and buccal epithelial cells (Zhao *et al.* 2007). To test this prediction, qRT-PCR was used to measure expression levels of seven adhesin genes (*ALS1*, *ALS5*, *ALS7*, *EAP1*, *HWP2*, *HYR1*, and *IFF4*) in wild-type *Candida* and low-virulence (*als7*Δ*als5*Δ) and high-virulence (*als3*Δ*hwp2*Δ) mutants. In addition to their phenotypes associated with virulence in the *C. elegans* liquid infection assay, these two mutants were further selected based on the highest (*als7*Δ*als5*Δ, 2,002 CFU/worm) and the lowest (*als3*Δ*hwp2*Δ, 1,060 CFU/worm) ability to colonize *C. elegans*, respectively. Expression levels were measured for each strain using both liquid- and agar-based conditions.

Overall, we found that adhesin expression patterns tend to be influenced by the infection environment. Adhesin expression on agar and in liquid was significantly different for wild-type fungi or the *als3*Δ*hwp2*Δ mutant (*i.e.* high-virulence strains), but not in the low-virulence mutant *als7*Δ*als5*Δ (Figure 4, A–C). Interestingly, of the adhesins measured, *ALS1* and *ALS5* showed the highest expression in wild type (Figure 4A), but their expression in the mutant strains was even higher when compared to the other adhesins (Figure 4, B and C). This outcome was surprising, as *ALS1* and *ALS5* were deleted from multiple mutants that retain the ability to efficiently colonize worms (*als7*Δ*als5*Δ, *hyr1*Δ*als1*Δ, and *iff4*Δ*als1*Δ). This suggests that either these adhesins do not play a prominent role in colonization, or one or more other genes compensate for their loss, making them redundant. Next, we compared expression for all four adhesin genes from *als3*Δ*hwp2*Δ and *als7*Δ*als5*Δ mutants under liquid conditions, where significant differences in colonization were observed. No significant differences for specific adhesins, nor the panel overall, were observed (Figure 4D). These findings likely indicated that the ability to colonize *C. elegans*' intestine is the outcome of expression of multiple adhesins. We also observed that adhesin expression is dependent on genotype, as expression levels of adhesin panel genes differed significantly between wild-type and mutant strains, regardless of media condition ($p < 0.0001$, for each comparison). Therefore, these data further support previous conclusions that, like bacterial pathogenesis assays, microbial physiology (as determined by growth media) can have a profound impact on pathogen virulence.

Adhesin mutant strains are impaired in filamentation and biofilm formation

Following *in vivo* analysis of fungal virulence and colonization, we performed *in vitro* biofilm and filamentation assays to determine whether observed differences in fungal virulence and/or colonization could be ascribed to altered ability of adhesin mutant strains to form biofilm or undergo cellular morphogenesis. Therefore, we first performed *in vitro* biofilm growth assays of the wild-type strain, along with the three most virulent, and three least virulent adhesin mutant strains. While this mutant library had previously been screened for biofilm formation (Shapiro *et al.* 2018a), here, we grew biofilms in the same BHI media in which the *C. elegans* liquid infection assays were performed, in order to maintain similar conditions between these assays. The selected strains were allowed to form biofilms in flat bottom 96-well plates for 72 h, planktonic cells were removed, and metabolic activity of the remaining biofilm was measured via XTT and quantified by spectrophotometer readout at OD_{490}. With the exception of *als9*Δ*iff4*Δ, each of the adhesin mutant strains were found to have impaired biofilm formation compared with the wild-type strain (Figure 5A; $P < 0.0005$). Given the known role of adhesins in fungal adhesion and biofilm initiation and growth, it is expected that these mutant strains would likely be defective in biofilm

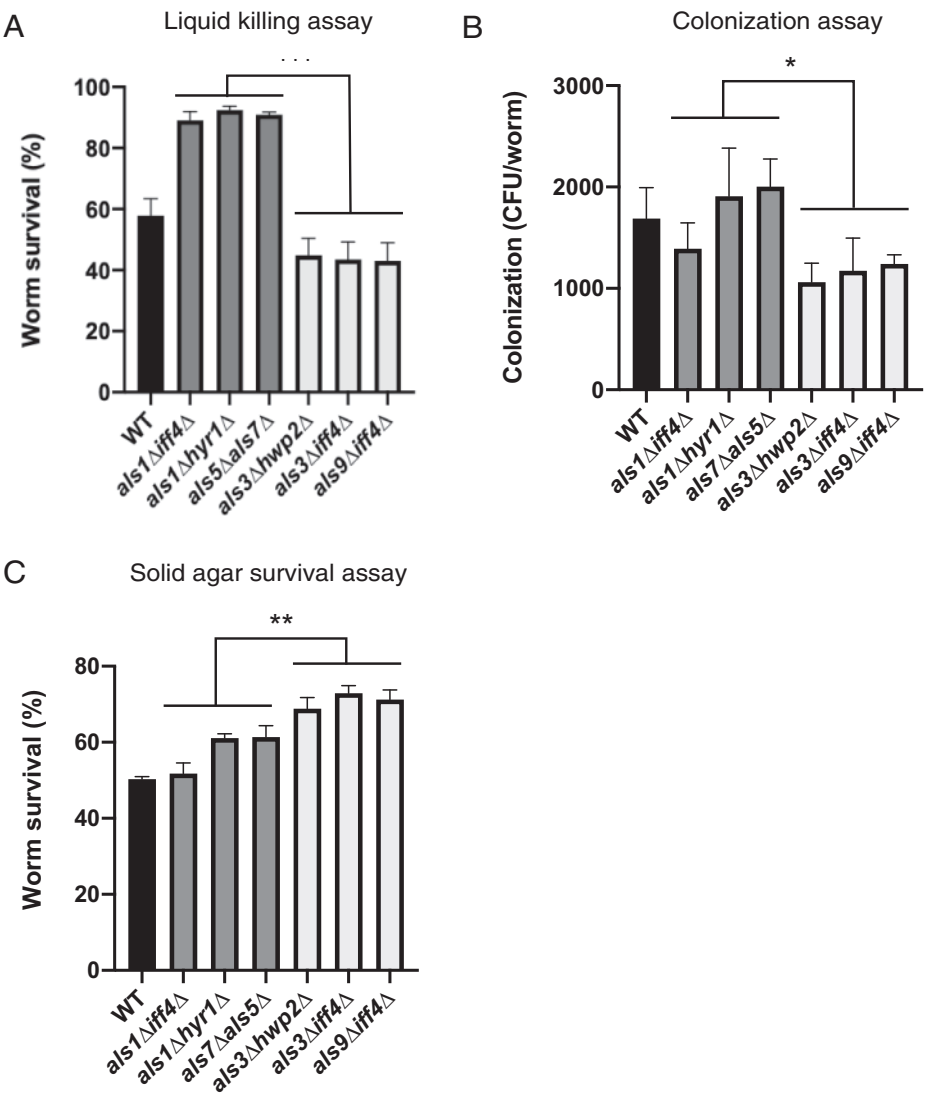

Figure 3 *C. albicans* mutants' virulence depends on infection model. *C. albicans* strains with the highest and lowest levels of virulence from our *C. elegans* infection screen were selected for follow-up analysis and monitored for worm colonization, as well as virulence in an agar plate infection model. (A) The three strains with lowest virulence (*als1*Δ*iff4*Δ, *hyr1*Δ*als5*Δ, *als7*Δ*als5*Δ; dark grey) and three with highest virulence (*als3*Δ*hwp2*Δ, *als3*Δ*iff4*Δ, *als9*Δ*iff4*Δ; light grey), based on the high-throughput *C. elegans* liquid media screen. Graph depicts the percent of worm survival. The three strains with lowest virulence were significantly different from the high-virulence strains $p < 0.0001$ for the pooled low- and high-virulence groups based on Student's *t*-test (***). (B) Ability of *C. albicans* mutant strains and wild type to colonize *C. elegans* worms was monitored. Colonization was assessed using colony-forming units (CFU) of *C. albicans* per worm. Lower virulence mutants (dark grey) had higher CFU/worm compared with higher virulence mutants (light grey) [$p < 0.05$ for the pooled low- and high-virulence groups based on Student's *t*-test (*)]. (C) An agar-based *C. elegans* infection model was used to compare data from the liquid-based infection screen. In this agar assay, *C. elegans* survival was scored daily until all the worms were dead. Graph depicts *C. elegans* survival data at day 4, at which point wild-type *C. albicans* has killed approximately 50% of worms. Low- and high-virulence mutants show a reverse trend from liquid assay, as strains that were highly virulent liquid killing had low pathogenesis on solid media, and vice versa [$p < 0.001$ for the pooled low- and high-virulence groups based on Student's *t*-test (**)]. All graphs were generated with GraphPad Prism. Error bars represent SEM.

growth. However, these results do not indicate a correlation between biofilm formation and virulence in our *C. elegans* liquid killing or agar-based assays, and suggest that mutants with reduced ability to form biofilms under these *in vitro* conditions are still capable of virulence in the *C. elegans* model of infection.

Selected mutants used in follow-up biofilm assays were also used in filamentation assays to assess the filamentation capabilities of adhesin mutants with variable virulence profiles. For this assay, wild-type and mutant strains were cultured in media with or without 10% serum, to induce filamentation in *C. albicans* cells. Each strain was imaged under phase microscopy and the percentage of filamentous cells (as a fraction of total cells) was calculated. Similar to what was observed with the biofilm growth assay, each of the adhesin mutant strains were found to have impaired ability to undergo morphogenesis and grow as filamentous cells, compared with the wild-type strain (Figure 5B; $p < 0.05$); although each of these mutants retains the ability to filament, they formed fewer filamentous cells compared with a wild-type strain, while retaining a similar growth rate to the wild type based on optical density (OD_{600}) measurements taken at the time of microscopic imaging. Representative microscopy of a low-virulence (*als7*Δ*als5*Δ) and high-virulence (*als9*Δ*iff4*Δ) strain indicate that both low- and high-virulence adhesin mutants are impaired in filamentous growth compared with a wild-type strain, when grown in the presence of serum (Figure 5C). The role of adhesins in mediating *C. albicans* filamentation has been less well-studied

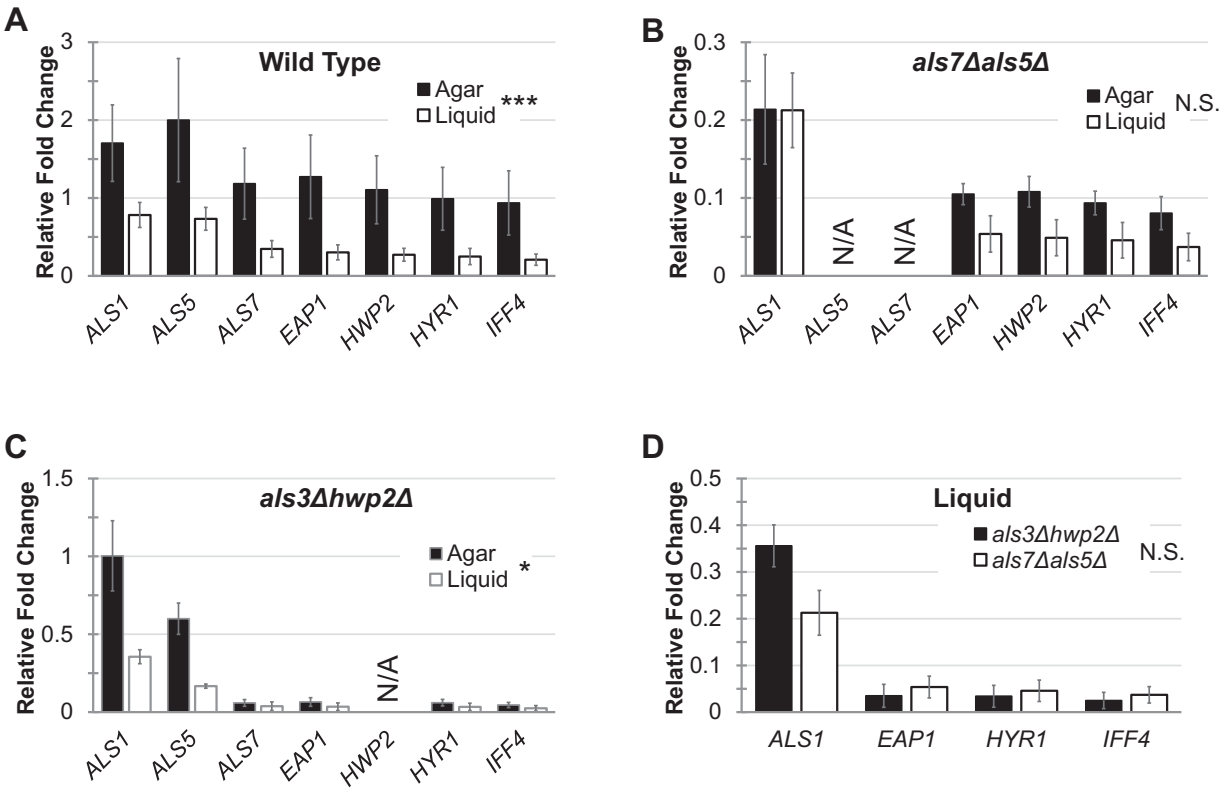

Figure 4 Adhesin gene expression patterns are affected by media conditions and genotype. qRT-PCR was used to measure expression levels of seven adhesin genes (*ALS1*, *ALS5*, *ALS7*, *EAP1*, *HWP2*, *HYR1*, and *IFF4*) for wild-type and representative low-virulence, high-colonization (*als7Δals5Δ*) or high-virulence, low-colonization (*als3Δhwp2Δ*) mutants. Expression levels were measured for each strain under both liquid and agar conditions. Relative expression of adhesin panel (measured relative to the housekeeping gene *ACT1*) in wild-type (A) and high-colonization, low-virulence (*als7Δals5Δ*) (B) or high-virulence, low-colonization (*als3Δhwp2Δ*) (C) mutants, under liquid or solid growth conditions. (D) Relative adhesin expression in liquid condition in selected mutants. Error bars represent SEM. ***$p < 0.001$, *$p < 0.05$, N.S. $p > 0.05$ according to Student's *t*-test for the overall panel.

compared with biofilm formation. These data suggest that deleting adhesin factors results in reduced ability to form filamentous cells, but similar to biofilm formation, is not correlated with virulence in our *C. elegans* liquid or agar infection assays. The lack of correlation between biofilm formation and virulence defects amongst *C. albicans* genetic mutant strains is in line with previous observations of transcription factor mutants (Nobile and Mitchell 2005; Pukkila-Worley *et al.* 2009).

Genetic interaction analysis identifies negative interactions between ALS5 and EAP1, as well as ALS5 and HWP2 in *C. albicans*

In addition to identifying the most virulent and avirulent adhesin mutants, we further wanted to characterize any potential genetic interactions between adhesin genes. Genetic interaction analysis would allow us to identify significant positive and negative genetic interactions, which point toward important synergies between these adhesin factors. Therefore, we performed genetic interaction analysis on our *C. albicans*–*C. elegans* virulence datasets, which compares virulence of double mutant deletion strain to that of their single mutant counterparts (*i.e.* *aΔbΔ* virulence compared to *aΔ* virulence and *bΔ* virulence). We used the commonly employed multiplicative model of genetic interactions (Boone *et al.* 2007; Baryshnikova *et al.* 2013; Halder *et al.* 2019), which predicts that the fitness of a double mutant will be the product of the fitness of each single mutant counterpart. Double mutant strains found to be less fit than predicted are said to have a negative genetic interaction, and those with higher fitness have a positive genetic interaction. For our assay, negative genetic interactions are particularly interesting, as it suggests deleting two adhesins in combination may lead to significantly reduced virulence—more than would be expected by deletion of either single adhesin on its own.

We used a simple program to assess genetic interactions and compare each double adhesin deletion mutant to its single mutant counterparts. First, for each replicate of the virulence screen, we normalized each mutant to the wild-type strain in order to obtain a relative virulence score. We then used these relative fitness measurements to calculate a predicted interaction score for each double mutant, based on the multiplicative model. Each predicted score was compared to the double mutant scores for both reciprocal pairs in each of the six replicate assays, and *t*-tests were used to compare the experimental values and the predicted values and determine whether we would reject the null hypothesis that there is no difference between the two (Figure 6A). We found two double mutants to have a significant negative genetic interaction: *als5Δeap1Δ* and *als5Δhwp2Δ* (Figure 6, A and B, $p < 0.05$). This indicates that deletions of *als5Δ* and *eap1Δ*, or *als5Δ* and *hwp2Δ* together, renders *C. albicans* significantly less virulent than deletion of *als5Δ*, *eap1Δ*, or *hwp2Δ* on their own, and that these factors act synergistically to promote fungal virulence in this *C. elegans* infection model. Interestingly, no significant positive genetic interactions were identified in this dataset.

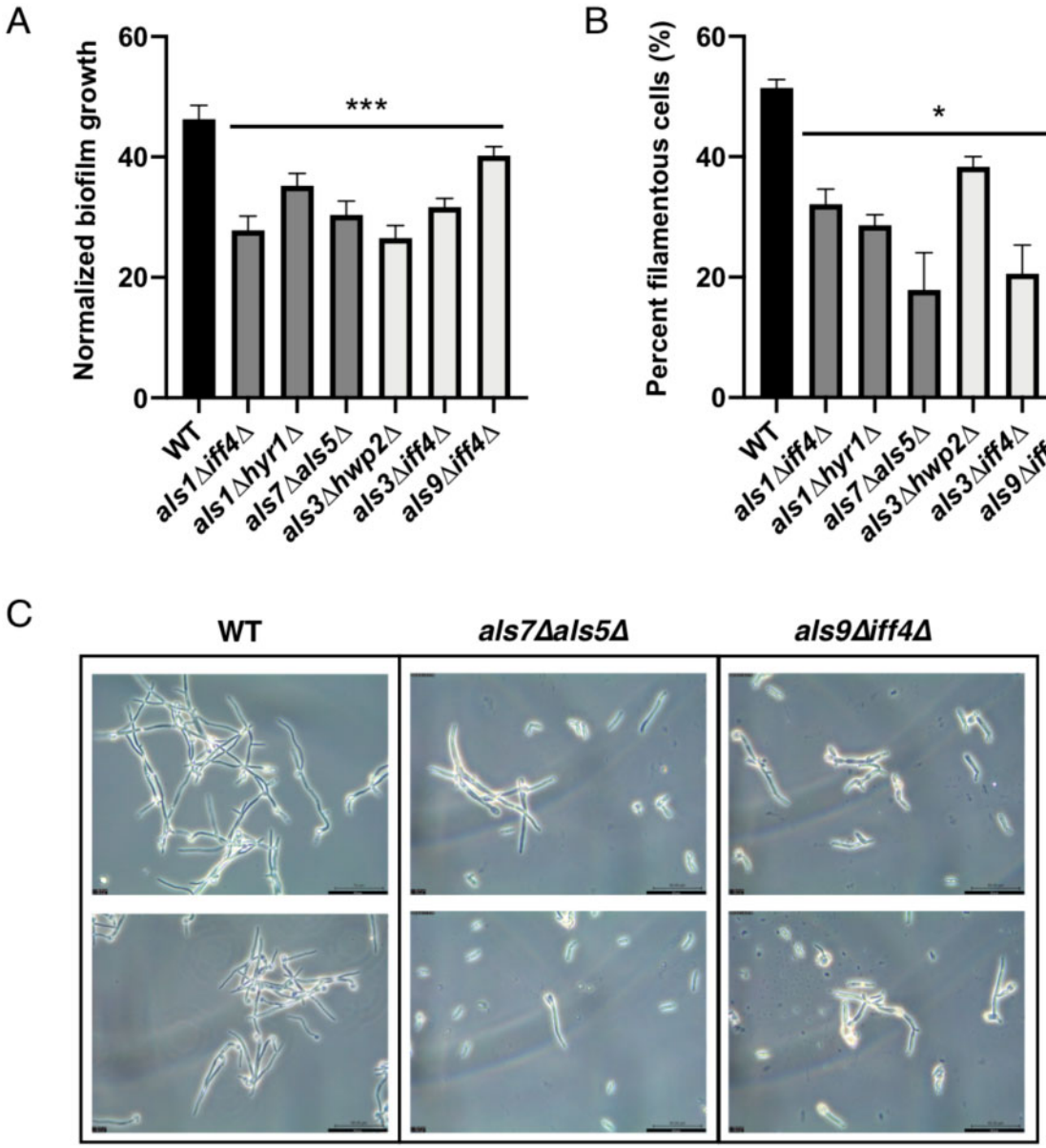

Figure 5 Adhesin mutant strains are deficient in filamentation and biofilm growth. The three strains with lowest virulence (*als1*Δ*iff4*Δ, *hyr1*Δ*als5*Δ, *als7*Δ*als5*Δ) and three with highest virulence (*als3*Δ*hwp2*Δ, *als3*Δ*iff4*Δ, *als9*Δ*iff4*Δ), based on the high-throughput *C. elegans* liquid media screen, have reduced ability to undergo morphogenesis or form biofilms, regardless of virulence phenotype. (A) Lowest virulence strains (*als1*Δ*iff4*Δ, *hyr1*Δ*als5*Δ, *als7*Δ*als5*Δ; dark grey) and highest virulence strains (*als3*Δ*hwp2*Δ, *als3*Δ*iff4*Δ, *als9*Δ*iff4*Δ; light grey), all have reduced ability to form biofilms compared to a wild-type strain (ANOVA, $p < 0.0005$ (***)). Biofilm growth was quantified by an XTT metabolic readout, measured at OD_{490} and normalized to planktonic growth. (B) Lowest virulence strains (*als1*Δ*iff4*Δ, *hyr1*Δ*als5*Δ, *als7*Δ*als5*Δ; dark grey) and highest virulence strains (*als3*Δ*hwp2*Δ, *als3*Δ*iff4*Δ, *als9*Δ*iff4*Δ; light grey), all have reduced ability to form filamentous cells [ANOVA, $p < 0.05$ (*)]. *C. albicans* cells were grown in media containing 10% FBS at 37°C to induce filamentation, and cells were counted using brightfield microscopy to determine the percentage of filamentous cells in the population. (C) Examples of reduced filamentation in a lower virulence (*als7*Δ*als5*Δ) and higher virulence (*als9*Δ*iff4*Δ) mutant strain. *C. albicans* cells were grown in media containing 10% FBS at 37°C to induce filamentation, and cells were counted using brightfield microscopy. Two representative microscopy images are shown for each strain at 40X magnification, scale bar is 50 μm.

Finally, we assessed whether these two genetic interaction mutants (*als5*Δ*eap1*Δ and *als5*Δ*hwp2*Δ) were impaired in filamentation and biofilm formation, compared with their counterpart single mutant strains. We performed a biofilm growth assay with each of these mutants, and found that while the single mutant strains (*als5*Δ, *eap1*Δ, and Δ*hwp2*Δ) as well as the double mutant strains (*als5*Δ*eap1*Δ and *als5*Δ*hwp2*Δ) were all impaired in biofilm formation, compared to the wild-type strain (Figure 6C, $p < 0.05$), the double mutants were not further deficient in biofilm growth compared to their single mutant counterpart strains. Similarly, all single and double mutant strains were significantly impaired in filamentation compared to the wild-type strain (Figure 6D, $p < 0.005$), yet the double mutants were not further deficient in filamentation growth compared to their single mutant counterpart strains, and in fact filamented more robustly than their single mutant counterparts. This suggests an uncoupling between filamentation, biofilm formation, and virulence, and/or further indicates how specific environmental conditions may influence the requirement for different adhesin proteins.

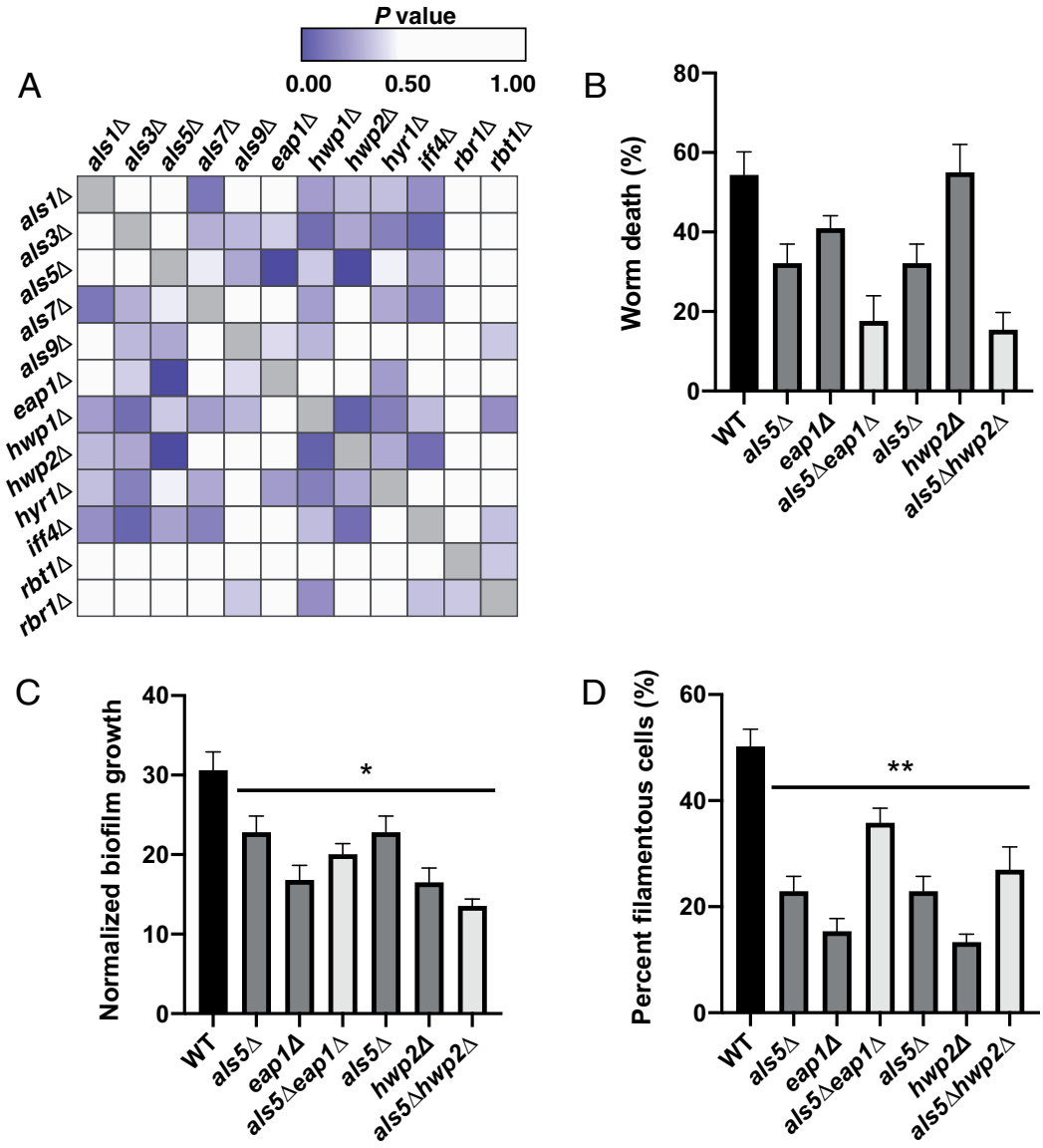

Figure 6 Genetic interaction analysis of adhesin mutant strains. Genetic interaction analysis was performed for all adhesin mutant strains to identify and characterize genetic interactions. (A) Summary of genetic interactions between each of the double mutant adhesin strains. A multiplicative model of genetic interactions was used to identify interactions where the double mutant strain virulence (fraction of dead worms) deviated from the predicted virulence based on the product of the two corresponding single mutants. The heatmap shows *p*-values for each double mutant genotype (reciprocal pairs were considered together as a single genotype), based on actual vs. predicted virulence measures across the six replicate experimental infection assays. Darker blue/purple represents lower *p*-values, and white represents higher values. Two mutants (*als5Δeap1Δ* and *als5Δhwp2*) were identified as significant interactions with $p < 0.05$. The heat map was generated using Morpheus matrix visualization and analysis software from the Broad Institute (https://software.broadinstitute.org/morpheus). (B) The virulence (percent worm death) of the two genetic interaction mutants (light grey), compared with their single mutant constituent mutants (dark grey) as well as the wild-type strain, based on the high-throughput *C. elegans* liquid media screen. Graph depicts the percent of worm death. (C) Each of the genetic interaction double mutants and their single mutant constituent strains have reduced ability to form biofilms compared to a wild-type strain [ANOVA, $p < 0.05$ (*)]. Biofilm growth was quantified by an XTT metabolic readout, measured at OD_{490} and normalized to planktonic growth. (D) Each of the genetic interaction double mutants and their single mutant constituent strains have reduced ability to form filamentous cells [ANOVA, $p < 0.005$ (**)]. *C. albicans* cells were grown in media containing 10% FBS at 37°C to induce filamentation, and cells were counted using brightfield microscopy to determine the percentage of filamentous cells in the population.

Discussion

Here, we present a systematic analysis of the role of adhesin factors, singly and in combinations, in *C. albicans* virulence. Our initial screening of 144 *C. albicans* strains exploited *C. elegans* as a model host uniquely suited for such high-throughput virulence analysis, and revealed single- and double-genetic mutant strains that retained high levels of virulence (comparable to wild type), and strains with significantly reduced levels of virulence. This screening platform was further able to identify genetic interactions between adhesin genes, and specific pairs of mutants that are significantly less virulent that would be expected based on the virulence of their single mutant constituent strains. This highlights the value in assessing virulence in higher-order genetic mutants, such as these double mutant libraries. In addition to screening for virulence, we followed up on strains with the highest and lowest levels of virulence. We found that *in vitro* measures of pathogenicity traits, including *C. albicans* filamentation, and biofilm formation were impaired in adhesin

mutant strains regardless of their virulence patterns in *C. elegans*, suggesting that under the conditions tested, filamentation and biofilm growth were uncoupled from virulence, which has been previously suggested (Pukkila-Worley *et al.* 2009; Noble *et al.* 2010). Furthermore, we found that mutants with less virulence in the *C. elegans* agar model were able to colonize these worms less well, compared with the more virulent strains, and that *C. elegans* survival upon *C. albicans* infection varied under different infection conditions (*i.e.* solid agar vs. liquid killing assays). Together, these data suggest a complex role of adhesin factors in mediating fungal virulence, and that specific environmental conditions have a critical role in influencing the requirement for different adhesin factors.

In this study, we were able to identify both combinations of adhesins, as well as single mutant adhesin strains with defects in virulence in a *C. elegans* model. Some of the single adhesin mutant strains have been previously identified as having a key role in virulence based on mammalian models of *C. albicans* infection. In our *C. elegans* liquid model, the *als1*Δ mutant strain had the most significant defect in virulence, and has similarly been implicated as a key mediator of virulence in a murine models of disseminated candidiasis (Alberti-Segui *et al.* 2004), a reconstituted human epithelium (RHE) model of oral candidiasis (Zhao *et al.* 2004), and a murine model of oropharyngeal candidiasis (Kamai *et al.* 2002). Other mutants with significant impairment in virulence in our *C. elegans* model, including *rbt1*Δ, have similarly been demonstrated to play a key role in virulence in mouse models of systemic *C. albicans* infection, as well as a rabbit cornea models of infection (Braun *et al.* 2000). In some cases, we found that mutants previously described to have significant impairment in virulence in animal models (*i.e.* *als3*Δ in RHE model of oral candidiasis and *hwp1*Δ in several mouse models of systemic and oropharyngeal candidiasis [Tsuchimori *et al.* 2000; Sundstrom *et al.* 2002a, 2002b]) had only modest defects in virulence in our *C. elegans* model, and in the case of *iff4*Δ [found to have decreased virulence in a murine intravenous infection model (Kempf *et al.* 2009)], we found essentially no defects in *C. elegans* virulence. Other single mutants, such as *als5*Δ, had significant virulence defects in our worm model, but have not been reported to have virulence defects in other animal models, to our knowledge. These observed differences and similarities between different adhesin mutants in their ability to cause virulence in distinct host models is likely due to the ligand or substrate binding specificity of these unique adhesin factors. *ALS1* and *ALS5*, for instance, which had the most significant role in virulence in our *C. elegans* model, are highly versatile adhesins with a demonstrated ability to recognize a very broad array of target ligands (Klotz *et al.* 2004), and adhere to numerous biotic and abiotic substrates (Gaur and Klotz 1997; Fu *et al.* 1998; Donohue *et al.* 2011b; Aoki *et al.* 2012; de Groot *et al.* 2013).

Host–pathogen interactions are complex and dynamic. In this manuscript, we demonstrated that *C. albicans* likely utilizes different virulence mechanisms in liquid- and agar-based assays. First, colonization on agar is higher than in liquid pathogenesis conditions (Supplementary Figure S3). Second, mutants with higher colonization (*als1*Δ*iff4*Δ, *als1*Δ*hyr1*Δ, and *als7*Δ*als5*Δ) are more virulent in an agar-based assay compared to mutants with lower colonization (*als3*Δ*hwp2*Δ, *als3*Δ*iff4*Δ, and *als9*Δ*iff4*Δ). At the same time, these higher colonization mutants have an approximately five-fold decrease in their ability to kill worms in the liquid-based assay. Interestingly, the same result was observed in the well-studied *C. elegans*–*P. aeruginosa* pathosystem, where multiple virulence models have been developed. For example, agar-based slow killing is characterized by high colonization of the host and the requirement for bacterial quorum sensing pathways for full virulence, with *lasR* and *gacA* mutants being low colonizers with attenuated virulence (Tan *et al.* 1999; Feinbaum *et al.* 2012). In contrast, liquid killing is characterized by low colonization, wild-type virulence of quorum-sensing mutants, and a requirement for the siderophore pyoverdine for full virulence (Kirienko *et al.* 2013, 2015; Kang *et al.* 2018). In this assay, multiple *pvd* mutants are attenuated, but no difference in colonization is observed between bacteria with low and wild-type virulence (Kirienko *et al.* 2013). This suggests that there may be a widespread correlation between colonization and virulence in agar assays but that correlation will be absent in liquid-based assays, where colonization is reduced.

The clear importance of different infection models and the broader pathogen environment on influencing fungal virulence, highlights the need to assess pathogenicity in different contexts. While mammalian models such as the mouse intravenous tail vein infection model for systemic candidiasis remain a gold standard for fungal virulence assays (Segal and Frenkel 2018), the simplicity of the *C. elegans* model and its tractability for high-throughput manipulation allowed us to rapidly screen a large library of adhesin mutants, and identify key regulators of virulence. Indeed, a breadth of previous research has exploited this model to study fungal virulence (Pukkila-Worley *et al.* 2009), the role of the antifungal host immune response (Pukkila-Worley *et al.* 2011, 2014), and antifungal drug efficacy (Breger *et al.* 2007; Okoli *et al.* 2009; Ewbank and Zugasti 2011) in *C. albicans*, and other fungal pathogens (Mylonakis *et al.* 2002a; Scorzoni *et al.* 2013). Other infection models that have been valuable for the study of *C. albicans* virulence include a *Drosophila* infection model (Alarco *et al.* 2004; Chamilos *et al.* 2006; Glittenberg *et al.* 2011; Wurster *et al.* 2019), and *Galleria mellonella* moth larvae model (Fuchs *et al.* 2010; Frenkel *et al.* 2016). Very recently, *Manduca sexta* caterpillars have been developed as a novel host model for the study of fungal virulence and drug efficacy (Lyons *et al.* 2020), which have several advantages over other nonmammalian models, including their ability to be maintained at 37°C and ability to assess fungal burden throughout the course of infection via the caterpillar's hemolymph of feces. Other recent work has identified a novel virulence phenotype to assess *Candida* pathogenesis in the *C. elegans* host model; this study found that in addition to causing host lethality, fungal pathogens such as *C. albicans* also reduce *C. elegans* fitness by delaying reproduction (Feistel *et al.* 2019). This has longer-term implications for overall *C. elegans* population growth, adds an important new layer to our understanding of this host–pathogen interaction, and may provide a more complete picture of virulence when studying fungal mutant strains, such as the adhesin mutants described here.

One of the unique capabilities of a high-throughput host–pathogen interaction model, is our ability to perform complex genetic interaction analysis. Genetic interaction analysis typically requires the analysis of single- and double-genetic mutant strains to compare double mutants to their single mutant counterparts, and often requires the analysis of numerous strains in order to identify significant interactions. While this work represents one of the first genetic interaction screens to monitor *C. albicans* virulence using an *in vivo* infection model, numerous other studies have probed the genetic interaction networks mediating pathogenesis traits in fungal pathogens (Bharucha *et al.* 2011; Diezmann *et al.* 2012; Usher *et al.* 2015; Glazier *et al.* 2017, 2018; Shapiro *et al.* 2018a; Glazier and Krysan 2020; Halder *et al.* 2020), as well as numerous bacterial pathogens (Joshi *et al.* 2006;

van Opijnen *et al.* 2009; Côté *et al.* 2016; Skwark *et al.* 2017), and parasites (Fang *et al.* 2018). Genetic interaction analysis in microbial pathogens has similarly been used as a means to probe complex genetic networks mediating host–pathogen interactions (O'Connor *et al.* 2012; Urbanus *et al.* 2016; Lee *et al.* 2019). While our CRISPR-based gene drive system enables such genetic interaction analysis in *C. albicans*, a caveat of this system is the potential for off-target mutations from the integrated CRISPR-Cas9 plasmid, which has been highlighted as a limitation of CRISPR systems in fungi and numerous other organisms (Hsu *et al.* 2013; Mitchell 2017; Song *et al.* 2019; Uthayakumar *et al.* 2021). Our previous whole-genome sequencing analysis (Shapiro *et al.* 2018a) had revealed that the gene drive system was specific with regards to gene deletions, but was not able to take into account possible off-target mutations and indels, which is a limitation of this specific platform.

In addition to using genetic interaction analysis as a means to understand genetic networks, genetic interaction analysis can also be exploited as a means to uncover novel pairs of cellular targets for combination antimicrobial therapeutics (Halder *et al.* 2020). In particular, synthetic lethal interactions, where mutation of two genes in combination is lethal to the cell while deletion of either gene on its own remains viable, can be used to identify targets for combination drug therapies (Cokol *et al.* 2011). Such genetic interaction-based approaches have been well validated for combination therapies for cancer (Han *et al.* 2017), as well as for antimicrobial therapeutics (Cheng *et al.* 2014; Pasquina *et al.* 2016; Usher and Haynes 2019). While our work does not identify lethal genetic combinations, we have identified genetic combinations that significantly impair virulence, more than would be expected by mutating the constituent single genes. Targeting virulence regulators, which impair a pathogen's ability to cause infection without altering its overall fitness, is gaining momentum as a potentially effective strategy for antimicrobial therapy (Cegelski *et al.* 2008; Maura *et al.* 2016; Dickey *et al.* 2017). Such "antivirulence" agents have been identified that inhibit pathogenicity traits such as morphogenesis and biofilm formation in *C. albicans* (Toenjes *et al.* 2005; Fazly *et al.* 2013; Romo *et al.* 2017; Vila *et al.* 2017; Garcia *et al.* 2018). Our work lends an understanding to new combinations of adhesins that significantly impair fungal virulence, suggesting new putative targets for combination antivirulence therapeutics.

Acknowledgments

We would like to thank the members of the Shapiro lab and the Kirienko lab for their hard work and assistance. We are thankful to Kieran Shah for his help writing the genetic interaction analysis script and to Anastasia Baryshnikova for helpful discussions.

Funding

Funding for this research was provided by grants from the Canadian Institutes for Health Research (CIHR), and the Natural Sciences and Engineering Research Council (NSERC) to R.S.S., a Mitacs Globalink Research Award to R.S.S. and S.R., a University of Guelph, College of Biological Science CBS Undergraduate Summer Research Assistantship Award to G.H.K., and a Welch Foundation and a John S. Dunn Foundation Award to N.V.K.

Conflicts of interest

None declared.

Literature cited

Aballay A, Ausubel FM. 2002. *Caenorhabditis elegans* as a host for the study of host–pathogen interactions. Curr Opin Microbiol. **5**: 97–101.

Ahamefule CS, Qin Q, Odiba AS, Li S, Moneke AN, *et al.* 2020. *Caenorhabditis elegans*-based *Aspergillus fumigatus* infection model for evaluating pathogenicity and drug efficacy. Front Cell Infect Microbiol. **10**:320.

Alarco A-M, Marcil A, Chen J, Suter B, Thomas D, *et al.* 2004. Immune-deficient *Drosophila melanogaster*: a model for the innate immune response to human fungal pathogens. J Immunol. **172**: 5622–5628.

Alberti-Segui C, Morales AJ, Xing H, Kessler MM, Willins DA, *et al.* 2004. Identification of potential cell-surface proteins in *Candida albicans* and investigation of the role of a putative cell-surface glycosidase in adhesion and virulence. Yeast. **21**:285–302.

Almeida RS, Brunke S, Albrecht A, Thewes S, Laue M, *et al.* 2008. The hyphal-associated adhesin and invasin Als3 of *Candida albicans* mediates iron acquisition from host ferritin. PLoS Pathog. **4**: e1000217.

Anderson QL, Revtovich AV, Kirienko NV. 2018. A High-throughput, high-content, liquid-based *C. elegans* pathosystem. J Vis Exp. 1: 58068. https://doi.org/10.3791/58068

Aoki W, Kitahara N, Miura N, Morisaka H, Kuroda K, *et al.* 2012. Profiling of adhesive properties of the agglutinin-like sequence (*ALS*) protein family, a virulent attribute of *Candida albicans*. FEMS Immunol Med Microbiol. **65**:121–124.

Babu M, Díaz-Mejía JJ, Vlasblom J, Gagarinova A, Phanse S, *et al.* 2011. Genetic interaction maps in *Escherichia coli* reveal functional crosstalk among cell envelope biogenesis pathways. PLoS Genet. **7**:e1002377.

Baryshnikova A, Costanzo M, Myers CL, Andrews B, Boone C. 2013. Genetic interaction networks: toward an understanding of heritability. Annu Rev Genomics Hum Genet. **14**:111–133.

Bharucha N, Chabrier-Rosello Y, Xu T, Johnson C, Sobczynski S, *et al.* 2011. A large-scale complex haploinsufficiency-based genetic interaction screen in *Candida albicans*: analysis of the RAM network during morphogenesis. PLoS Genet. **7**:e1002058.

Bongomin F, Gago S, Oladele R, Denning D. 2017. Global and multi-national prevalence of fungal diseases—estimate precision. J Fungi (Basel). **3**:57.

Boone C, Bussey H, Andrews BJ. 2007. Exploring genetic interactions and networks with yeast. Nat Rev Genet. **8**:437–449.

Braun BR, Head WS, Wang MX, Johnson AD. 2000. Identification and characterization of *TUP1*-regulated genes in *Candida albicans*. Genetics. **156**:31–44.

Breger J, Fuchs BB, Aperis G, Moy TI, Ausubel FM, *et al.* 2007. Antifungal chemical compounds identified using a *C. elegans* pathogenicity assay. PLoS Pathog. **3**:e18.

Butland G, Babu M, Díaz-Mejía JJ, Bohdana F, Phanse S, *et al.* 2008. eSGA: *E. coli* synthetic genetic array analysis. Nat Methods. **5**: 789–795.

C. elegans Sequencing Consortium 1998. Genome sequence of the nematode *C. elegans*: a platform for investigating biology. Science. **282**:2012–2018. [10.1126/science.282.5396.2012]

Calderone RA, Braun PC. 1991. Adherence and receptor relationships of *Candida albicans*. Microbiol Rev. **55**:1–20.

Cegelski L, Marshall GR, Eldridge GR, Hultgren SJ. 2008. The biology and future prospects of antivirulence therapies. Nat Rev Microbiol. **6**:17–27.

Chamilos G, Lionakis MS, Lewis RE, Lopez-Ribot JL, Saville SP, *et al.* 2006. *Drosophila melanogaster* as a facile model for large-scale

studies of virulence mechanisms and antifungal drug efficacy in *Candida* species. J Infect Dis. **193**:1014–1022.

Cheng AA, Ding H, Lu TK. 2014. Enhanced killing of antibiotic-resistant bacteria enabled by massively parallel combinatorial genetics. Proc Natl Acad Sci USA. **111**:12462–12467.

Cleary IA, Reinhard SM, Miller CL, Murdoch C, Thornhill MH, *et al.* 2011. *Candida albicans* adhesin Als3p is dispensable for virulence in the mouse model of disseminated candidiasis. Microbiology. **157**:1806–1815.

Cokol M, Chua HN, Tasan M, Mutlu B, Weinstein ZB, *et al.* 2011. Systematic exploration of synergistic drug pairs. Mol Syst Biol. **7**: 544.

Costanzo M, Baryshnikova A, Bellay J, Kim Y, Spear ED, *et al.* 2010. The genetic landscape of a cell. Science. **327**:425–431.

Costanzo M, VanderSluis B, Koch EN, Baryshnikova A, Pons C, *et al.* 2016. A global genetic interaction network maps a wiring diagram of cellular function. Science. **353**:aaf1420.

Côté J-P, French S, Gehrke SS, MacNair CR, Mangat CS, *et al.* 2016. The genome-wide interaction network of nutrient stress genes in *Escherichia coli*. MBio. **7**:e01714–16

Denning DW. 2017. Calling upon all public health mycologists. Eur J Clin Microbiol Infect Dis. **36**:923–924.

Dickey SW, Cheung GYC, Otto M. 2017. Different drugs for bad bugs: antivirulence strategies in the age of antibiotic resistance. Nat Rev Drug Discov. **16**:457–471.

Diezmann S, Michaut M, Shapiro RS, Bader GD, Cowen LE. 2012. Mapping the Hsp90 genetic interaction network in *Candida albicans* reveals environmental contingency and rewired circuitry. PLoS Genet. **8**:e1002562.

Dixon SJ, Costanzo M, Baryshnikova A, Andrews B, Boone C. 2009. Systematic mapping of genetic interaction networks. Annu Rev Genet. **43**:601–625.

Donohue DS, Ielasi FS, Goossens KVY, Willaert RG. 2011a. The N-terminal part of Als1 protein from *Candida albicans* specifically binds fucose-containing glycans. Mol Microbiol. **80**:1667–1679.

Donohue DS, Ielasi FS, Goossens KVY, Willaert RG. 2011b. The N-terminal part of Als1 protein from *Candida albicans* specifically binds fucose-containing glycans. Mol Microbiol. **80**:1667–1679.

Elkabti AB, Issi L, Rao RP. 2018. *Caenorhabditis elegans* as a model host to monitor the *Candida* infection processes. J Fungi (Basel) 4:123.

Ermolaeva MA, Schumacher B. 2014. Insights from the worm: the *C. elegans* model for innate immunity. Semin Immunol. **26**:303–309.

Evans EA, Chen WC, Tan M-W. 2008. The DAF-2 insulin-like signaling pathway independently regulates aging and immunity in *C. elegans*. Aging Cell. **7**:879–893.

Ewbank JJ, Zugasti O. 2011. *C. elegans*: model host and tool for antimicrobial drug discovery. Dis Model Mech. **4**:300–304.

Fang H, Gomes AR, Klages N, Pino P, Maco B, *et al.* 2018. Epistasis studies reveal redundancy among calcium-dependent protein kinases in motility and invasion of malaria parasites. Nat Commun. **9**:4248.

Fazly A, Jain C, Dehner AC, Issi L, Lilly EA, *et al.* 2013. Chemical screening identifies filastatin, a small molecule inhibitor of *Candida albicans* adhesion, morphogenesis, and pathogenesis. Proc Natl Acad Sci USA. **110**:13594–13599.

Feinbaum RL, Urbach JM, Liberati NT, Djonovic S, Adonizio A, *et al.* 2012. Genome-wide identification of *Pseudomonas aeruginosa* virulence-related genes using a *Caenorhabditis elegans* infection model. PLoS Pathog. **8**:e1002813.

Feistel DJ, Elmostafa R, Nguyen N, Penley M, Morran L, *et al.* 2019. A novel virulence phenotype rapidly assesses *Candida* fungal pathogenesis in healthy and immunocompromised *Caenorhabditis elegans* hosts. mSphere. **4**:e006976.

Finkel JS, Mitchell AP. 2011. Genetic control of *Candida albicans* biofilm development. Nat Rev Microbiol. **9**:109–118.

Fisher MC, Gurr SJ, Cuomo CA, Blehert DS, Jin H, *et al.* 2020. Threats posed by the fungal kingdom to humans, wildlife, and agriculture. MBio. **11**:e00449.

Frenkel M, Mandelblat M, Alastruey-Izquierdo A, Mendlovic S, Semis R, *et al.* 2016. Pathogenicity of *Candida albicans* isolates from bloodstream and mucosal candidiasis assessed in mice and *Galleria mellonella*. J Mycol Med. **26**:1–8.

Fu Y, Ibrahim AS, Sheppard DC, Chen Y-C, French SW, *et al.* 2002. *Candida albicans* Als1p: an adhesin that is a downstream effector of the *EFG1* filamentation pathway. Mol Microbiol. **44**:61–72.

Fu Y, Rieg G, Fonzi WA, Belanger PH, Edwards JE, *et al.* 1998. Expression of the *Candida albicans* gene *ALS1* in *Saccharomyces cerevisiae* induces adherence to endothelial and epithelial Cells. Infect Immun. **66**:1783–1786.

Fuchs BB, O'Brien E, Khoury JBE, Mylonakis E. 2010. Methods for using *Galleria mellonella* as a model host to study fungal pathogenesis. Virulence. **1**:475–482.

Gallagher LA, Manoil C. 2001. *Pseudomonas aeruginosa* PAO1 kills *Caenorhabditis elegans* by cyanide poisoning. J Bacteriol. **183**: 6207–6214.

Garcia C, Burgain A, Chaillot J, Pic É, Khemiri I, *et al.* 2018. A phenotypic small-molecule screen identifies halogenated salicylanilides as inhibitors of fungal morphogenesis, biofilm formation and host cell invasion. Sci Rep. **8**:11559.

Garsin DA, Villanueva JM, Begun J, Kim DH, Sifri CD, *et al.* 2003. *Long-lived C. elegans* daf-2 mutants are resistant to bacterial pathogens. Science. **300**:1921–1921.

Gaur NK, Klotz SA. 1997. Expression, cloning, and characterization of a *Candida albicans* gene, *ALA1*, that confers adherence properties upon *Saccharomyces cerevisiae* for extracellular matrix proteins. Infect Immun. **65**:5289–5294.

Geddes-McAlister J, Shapiro RS. 2019. New pathogens, new tricks: emerging, drug-resistant fungal pathogens and future prospects for antifungal therapeutics. Ann N Y Acad Sci. **1435**: 57–78.

Glazier VE, Murante T, Koselny K, Murante D, Esqueda M, *et al.* 2018. Systematic complex haploinsufficiency-based genetic analysis of *Candida albicans* transcription factors: tools and applications to virulence-associated phenotypes. G3 (Bethesda). **8**:1299–1314.

Glazier VE, Murante T, Murante D, Koselny K, Liu Y, *et al.* 2017. Genetic analysis of the *Candida albicans* biofilm transcription factor network using simple and complex haploinsufficiency. PLoS Genet. **13**:e1006948.

Glazier VE, Krysan DJ. 2020. Genetic interaction analysis comes to the diploid human pathogen *Candida albicans*. PLoS Pathog. **16**: e1008399.

Glittenberg MT, Silas S, MacCallum DM, Gow NAR, Ligoxygakis P. 2011. Wild-type *Drosophila melanogaster* as an alternative model system for investigating the pathogenicity of *Candida albicans*. Dis Model Mech. **4**:504–514.

Gravato-Nobre MJ, Hodgkin J. 2005. *Caenorhabditis elegans* as a model for innate immunity to pathogens. Cell Microbiol. **7**:741–751.

Groot PWJD, Bader O, de Boer AD, Weig M, Chauhan N. 2013. Adhesins in human fungal pathogens: glue with plenty of stick. Eukaryot Cell **12**:470–481.

Halder V, McDonnell B, Uthayakumar D, Usher J, Shapiro RS. 2020. Genetic interaction analysis in microbial pathogens: unravelling networks of pathogenesis, antimicrobial susceptibility and host interactions. FEMS Microbiol Rev. doi: 10.1093/femsre/fuaa055.

Halder V, Porter CBM, Chavez A, Shapiro RS. 2019. Design, execution, and analysis of CRISPR–Cas9-based deletions and genetic

interaction networks in the fungal pathogen *Candida albicans*. Nat Protoc. **14**:955–975.

Han K, Jeng EE, Hess GT, Morgens DW, Li A, *et al.* 2017. Synergistic drug combinations for cancer identified in a CRISPR screen for pairwise genetic interactions. Nat Biotechnol. **35**:463–474.

Hernando-Ortiz A, Mateo E, Ortega-Riveros De-la-Pinta MI, Quindós G, *et al.* 2020. *Caenorhabditis elegans* as a model system to assess *Candida glabrata*, *Candida nivariensis* and *Candida bracarensis* virulence and antifungal efficacy. Antimicrob Agents Chemother. **64**: e00824. https://doi.org/10.1128/AAC.00824-20

Hoyer LL. 2001. The *ALS* gene family of *Candida albicans*. Trends Microbiol. **9**:176–180.

Hoyer LL, Cota E. 2016. *Candida albicans* agglutinin-like sequence (Als) family vignettes: a review of Als protein structure and function. Front Microbiol. **7**:280.

Hoyer LL, Green CB, Oh S-H, Zhao X. 2008. Discovering the secrets of the *Candida albicans* agglutinin-like sequence (*ALS*) gene family–a sticky pursuit. Med Mycol. **46**:1–15.

Hoyer LL, Payne TL, Bell M, Myers AM, Scherer S. 1998. *Candida albicans ALS3* and insights into the nature of the *ALS* gene family. Curr Genet. **33**:451–459.

Hsu PD, Scott DA, Weinstein JA, Ran FA, Konermann S, *et al.* 2013. DNA targeting specificity of RNA-guided Cas9 nucleases. Nat Biotechnol. **31**:827–832.

Huang X, Li D, Xi L, Mylonakis E. 2014. *Caenorhabditis elegans*: a simple nematode infection model for *Penicillium marneffei*. PLoS One. **9**: e108764.

Ibrahim AS, Spellberg BJ, Avenissian V, Fu Y, Filler SG, *et al.* 2005. Vaccination with recombinant N-terminal domain of Als1p improves survival during murine disseminated candidiasis by enhancing cell-mediated, not humoral. Infect Immun. **73**: 999–1005.

Irazoqui JE, Urbach JM, Ausubel FM. 2010. Evolution of host innate defence: insights from *Caenorhabditis elegans* and primitive invertebrates. Nat Rev Immunol. **10**:47–58.

Issi L, Rioux M, Rao R. 2017. The nematode *Caenorhabditis elegans* - a versatile *in vivo* model to study host-microbe interactions. J Vis Exp. 56487.

Jain C, Pastor K, Gonzalez AY, Lorenz MC, Rao RP. 2013. The role of *Candida albicans* AP-1 protein against host derived ROS in in vivo models of infection. Virulence. **4**:67–76.

Joshi SM, Pandey AK, Capite N, Fortune SM, Rubin EJ, *et al.* 2006. Characterization of mycobacterial virulence genes through genetic interaction mapping. Proc Natl Acad Sci USA. **103**: 11760–11765.

Kamai Y, Kubota M, Kamai Y, Hosokawa T, Fukuoka T, *et al.* 2002. Contribution of *Candida albicans ALS1* to the pathogenesis of experimental oropharyngeal candidiasis. Infect Immun. **70**: 5256–5258.

Kang D, Kirienko DR, Webster P, Fisher AL, Kirienko NV. 2018. Pyoverdine, a siderophore from *Pseudomonas aeruginosa*, translocates into *C. elegans*, removes iron, and activates a distinct host response. Virulence. **9**:804–817.

Kempf M, Cottin J, Licznar P, Lefrançois C, Robert R, *et al.* 2009. Disruption of the GPI protein-encoding gene *IFF4* of *Candida albicans* results in decreased adherence and virulence. Mycopathologia. **168**:73–77.

Kim DH, Ausubel FM. 2005. Evolutionary perspectives on innate immunity from the study of *Caenorhabditis elegans*. Curr Opin Immunol. **17**:4–10.

Kim GH, Rosiana S, Kirienko NV, Shapiro RS. 2020. A simple nematode infection model for studying *Candida albicans* pathogenesis. Curr Protoc Microbiol. **59**:e114.

Kirienko DR, Kang D, Kirienko NV. 2019. Novel pyoverdine inhibitors mitigate *Pseudomonas aeruginosa* pathogenesis. Front Microbiol. **9**: 3317.

Kirienko DR, Revtovich AV, Kirienko NV. 2016. A high-content, phenotypic screen identifies fluorouridine as an inhibitor of pyoverdine biosynthesis and *Pseudomonas aeruginosa* virulence. mSphere. **1**:e00217-16.

Kirienko NV, Ausubel FM, Ruvkun G. 2015. Mitophagy confers resistance to siderophore-mediated killing by *Pseudomonas aeruginosa*. Proc Natl Acad Sci USA. **112**:1821–1826.

Kirienko NV, Cezairliyan BO, Ausubel FM, Powell JR. 2014. *Pseudomonas aeruginosa* PA14 pathogenesis in *Caenorhabditis elegans*. Methods Mol Biol. **1149**:653–669.

Kirienko NV, Kirienko DR, Larkins-Ford J, Wählby C, Ruvkun G, *et al.* 2013. *Pseudomonas aeruginosa* disrupts *Caenorhabditis elegans* iron homeostasis, causing a hypoxic response and death. Cell Host Microbe. **13**:406–416.

Klotz SA, Gaur NK, Lake DF, Chan V, Rauceo J, *et al.* 2004. Degenerate peptide recognition by *Candida albicans* adhesins Als5p and Als1p. Infect Immun. **72**:2029–2034.

Kullberg BJ, Arendrup MC. 2016. Invasive candidiasis. N Engl J Med. **374**:794–795.

Kumar A, Baruah A, Tomioka M, Iino Y, Kalita MC, *et al.* 2020. *Caenorhabditis elegans*: a model to understand host–microbe interactions. Cell Mol Life Sci. **77**:1229–1249.

Lee AH-Y, Bastedo DP, Youn J-Y, Lo T, Middleton MA, *et al.* 2019. Identifying *Pseudomonas syringae* type III secreted effector function via a yeast genomic screen. G3 (Bethesda). **9**:535–547. [10.1534/g3.118.200877]

Lipke PN. 2018. What we do not know about fungal cell adhesion molecules. J Fungi (Basel). **4**:59.

Lohse MB, Gulati M, Johnson AD, Nobile CJ. 2018. Development and regulation of single- and multi-species *Candida albicans* biofilms. Nat Rev Microbiol. **16**:19–31.

Lyons N, Softley I, Balfour A, Williamson C, O'Brien HE, *et al.* 2020. Tobacco Hornworm (*Manduca sexta*) caterpillars as a novel host model for the study of fungal virulence and drug efficacy. Virulence. **11**:1075–1089.

Mahajan-Miklos S, Tan MW, Rahme LG, Ausubel FM. 1999. Molecular mechanisms of bacterial virulence elucidated using a *Pseudomonas aeruginosa-Caenorhabditis elegans* pathogenesis model. Cell. **96**:47–56.

Marsh EK, May RC. 2012. *Caenorhabditis elegans*, a model organism for investigating immunity. Appl Environ Microbiol. **78**:2075–2081.

Maura D, Ballok AE, Rahme LG. 2016. Considerations and caveats in anti-virulence drug development. Curr Opin Microbiol. **33**:41–46.

Mayer FL, Wilson D, Hube B. 2013. *Candida albicans* pathogenicity mechanisms. Virulence. **4**:119–128.

McGhee J. 2007. WormBook: The *C. elegans* intestine. Pasadena. https://www.ncbi.nlm.nih.gov/books/NBK19717/.

Mitchell AP. 2017. Location, location, location: use of CRISPR-Cas9 for genome editing in human pathogenic fungi. PLoS Pathog. **13**: e1006209.

Moy TI, Conery AL, Larkins-Ford J, Wu G, Mazitschek R, *et al.* 2009. High-throughput screen for novel antimicrobials using a whole animal infection model. ACS Chem Biol. **4**:527–533.

Mylonakis E, Ausubel FM, Perfect JR, Heitman J, Calderwood SB. 2002a. Nonlinear partial differential equations and applications: killing of *Caenorhabditis elegans* by *Cryptococcus neoformans* as a model of yeast pathogenesis. Proc Natl Acad Sci USA. **99**: 15675–15680.

Mylonakis E, Ausubel FM, Perfect JR, Heitman J, Calderwood SB. 2002b. Killing of *Caenorhabditis elegans* by *Cryptococcus neoformans*

as a model of yeast pathogenesis. Proc Natl Acad Sci USA. **99**: 15675–15680.

Nobile CJ, Johnson AD. 2015. *Candida albicans* biofilms and human disease. Annu Rev Microbiol. **69**:71–92.

Nobile CJ, Mitchell AP. 2005. Regulation of cell-surface genes and biofilm formation by the *C. albicans* transcription factor Bcr1p. Curr Biol. **15**:1150–1155.

Nobile CJ, Schneider HA, Nett JE, Sheppard DC, Filler SG, *et al.* 2008. Complementary adhesin function in *C. albicans* biofilm formation. Curr Biol. **18**:1017–1024.

Noble SM, French S, Kohn LA, Chen V, Johnson AD. 2010. Systematic screens of a *Candida albicans* homozygous deletion library decouple morphogenetic switching and pathogenicity. Nat Genet. **42**: 590–598.

Norris AD, Gracida X, Calarco JA. 2017. CRISPR-mediated genetic interaction profiling identifies RNA binding proteins controlling metazoan fitness. Elife. **6**:e28129.

O'Connor TJ, Boyd D, Dorer MS, Isberg RR. 2012. Aggravating genetic interactions allow a solution to redundancy in a bacterial pathogen. Science. **338**:1440–1444.

Okoli I, Coleman JJ, Tempakakis E, An WF, Holson E, *et al.* 2009. Identification of antifungal compounds active against *Candida albicans* using an improved high-throughput *Caenorhabditis elegans* assay. PLoS One. **4**:e7025.

Opijnen TV, Bodi KL, Camilli A. 2009. Tn-seq: high-throughput parallel sequencing for fitness and genetic interaction studies in microorganisms. Nat Methods. **6**:767–772.

Pasquina L, Santa Maria JP, Jr, McKay Wood B, Moussa SH, Matano LM, *et al.* 2016. A synthetic lethal approach for compound and target identification in *Staphylococcus aureus*. Nat Chem Biol. **12**: 40–45.

Pfaller MA, Diekema DJ. 2007. Epidemiology of invasive candidiasis: a persistent public health problem. Clin Microbiol Rev. **20**: 133–163.

Phan QT, Myers CL, Fu Y, Sheppard DC, Yeaman MR, *et al.* 2007. Als3 is a *Candida albicans* invasin that binds to cadherins and induces endocytosis by host cells. PLoS Biol. **5**:e64.

Pukkila-Worley R, Peleg AY, Tampakakis E, Mylonakis E. 2009. *Candida albicans* hyphal formation and virulence assessed using a *Caenorhabditis elegans* infection model. Eukaryot Cell. **8**:1750–1758.

Pukkila-Worley R, Ausubel FM, Mylonakis E. 2011. *Candida albicans* infection of *Caenorhabditis elegans* induces antifungal immune defenses. PLoS Pathog. **7**:e1002074.

Pukkila-Worley R, Feinbaum RL, McEwan DL, Conery AL, Ausubel FM. 2014. The evolutionarily conserved mediator subunit MDT-15/MED15 links protective innate immune responses and xenobiotic detoxification. PLoS Pathog. **10**:e1004143.

Pukkila-Worley R, Mylonakis E. 2010. From the outside in and the inside out: Antifungal immune responses in *Caenorhabditis elegans*. Virulence. **1**:111–112.

Romo JA, Pierce CG, Chaturvedi AK, Lazzell AL, McHardy SF, *et al.* 2017. Development of anti-virulence approaches for candidiasis via a novel series of small-molecule inhibitors of *Candida albicans* filamentation. MBio. **8**:e01991–e01997.

Scorzoni L, de Lucas MP, Mesa-Arango AC, Fusco-Almeida AM, Lozano E, *et al.* 2013. Antifungal efficacy during *Candida krusei* infection in non-conventional models correlates with the yeast *in vitro* susceptibility profile. PLoS One. **8**:e60047.

Segal E, Frenkel M. 2018. Experimental *in vivo* models of candidiasis. J Fungi (Basel). **4**:21.

Shapiro RS, Chavez A, Collins JJ. 2018b. CRISPR-based genomic tools for the manipulation of genetically intractable microorganisms. Nat Rev Microbiol. **16**:333–339.

Shapiro RS, Chavez A, Porter CBM, Hamblin M, Kaas CS, *et al.* 2018a. A CRISPR-Cas9-based gene drive platform for genetic interaction analysis in *Candida albicans*. Nat Microbiol. **3**:73–82.

Shapiro RS, Robbins N, Cowen LE. 2011. Regulatory circuitry governing fungal development, drug resistance, and disease. Microbiol Mol Biol Rev. **75**:213–267.

Sharma J, Rosiana S, Razzaq I, Shapiro RS. 2019. Linking cellular morphogenesis with antifungal treatment and susceptibility in *Candida* pathogens. J Fungi (Basel). **5**:17.

Sheppard DC, Yeaman MR, Welch WH, Phan QT, Fu Y, *et al.* 2004. Functional and structural diversity in the Als protein family of *Candida albicans*. J Biol Chem. **279**:30480–30489.

Skwark MJ, Croucher NJ, Puranen S, Chewapreecha C, Pesonen M, *et al.* 2017. Interacting networks of resistance, virulence and core machinery genes identified by genome-wide epistasis analysis. PLoS Genet. **13**:e1006508.

Song R, Zhai Q, Sun L, Huang E, Zhang Y, *et al.* 2019. CRISPR/Cas9 genome editing technology in filamentous fungi: progress and perspective. Appl Microbiol Biotechnol. **103**:6919–6932.

Sudbery PE. 2011. Growth of *Candida albicans* hyphae. Nat Rev Microbiol. **9**:737–748.

Sundstrom P. 1999. Adhesins in *Candida albicans*. Curr Opin Microbiol. **2**:353–357.

Sundstrom P, Balish E, Allen CM. 2002a. Essential role of the *Candida albicans* transglutaminase substrate, hyphal wall protein 1, in lethal oroesophageal candidiasis in immunodeficient mice. J Infect Dis. **185**:521–530.

Sundstrom P, Cutler JE, Staab JF. 2002b. Reevaluation of the role of *HWP1* in systemic candidiasis by use of *Candida albicans* strains with selectable marker *URA3* targeted to the *ENO1* locus. Infect Immun. **70**:3281–3283.

Tan MW, Mahajan-Miklos S, Ausubel FM. 1999. Killing of *Caenorhabditis elegans* by *Pseudomonas aeruginosa* used to model mammalian bacterial pathogenesis. Proc Natl Acad Sci USA. **96**:715–720.

Tang RJ, Breger J, Idnurm A, Gerik KJ, Lodge JK, *et al.* 2005. *Cryptococcus neoformans* gene involved in mammalian pathogenesis identified by a *Caenorhabditis elegans* progeny-based approach. Infect Immun. **73**:8219–8225.

Toenjes KA, Munsee SM, Ibrahim AS, Jeffrey R, Edwards JE Jr, *et al.* 2005. Small-molecule inhibitors of the budded-to-hyphal-form transition in the pathogenic yeast *Candida albicans*. Antimicrob Agents Chemother. **49**:963–972.

Tsuchimori N, Sharkey LL, Fonzi WA, French SW, Edwards JE Jr, *et al.* 2000. Reduced virulence of *HWP1*-deficient mutants of *Candida albicans* and their interactions with host cells. Infect Immun. **68**: 1997–2002.

Tsui C, Kong EF, Jabra-Rizk MA. 2016. Pathogenesis of *Candida albicans* biofilm. Pathog Dis. **74**:ftw018.

Urbanus ML, Quaile AT, Stogios PJ, Morar M, Rao C, *et al.* 2016. Diverse mechanisms of metaeffector activity in an intracellular bacterial pathogen, *Legionella pneumophila*. Mol Syst Biol. **12**:893.

Usher J, Haynes K. 2019. Attenuating the emergence of anti-fungal drug resistance by harnessing synthetic lethal interactions in a model organism. PLoS Genet. **15**:e1008259.

Usher J, Thomas G, Haynes K. 2015. Utilising established SDL-screening methods as a tool for the functional genomic characterisation of model and non-model organisms. FEMS Yeast Res. **15**:fov091.

Utari PD, Quax WJ. 2013. *Caenorhabditis elegans* reveals novel *Pseudomonas aeruginosa* virulence mechanism. Trends Microbiol. **21**:315–316.

Uthayakumar D, Sharma J, Wensing L, Shapiro R. 2021. CRISPR-based genetic manipulation of *Candida* species: historical perspectives and current approaches. Front Genome Ed. **2**:31.

Vila T, Romo JA, Pierce CG, McHardy SF, Saville SP, *et al.* 2017. Targeting *Candida albicans* filamentation for antifungal drug development. Virulence. **8**:150–158.

Wurster S, Bandi A, Beyda ND, Albert ND, Raman NM, *et al.* 2019. *Drosophila melanogaster* as a model to study virulence and azole treatment of the emerging pathogen *Candida auris*. J Antimicrob Chemother. **74**:1904–1910.

Zaborin A, Romanowski K, Gerdes S, Holbrook C, Lepine F, *et al.* 2009. Red death in *Caenorhabditis elegans* caused by *Pseudomonas aeruginosa* PAO1. Proc Natl Acad Sci USA. **106**:6327–6332.

Zhao X, Oh S-H, Cheng G, Green CB, Nuessen JA, *et al.* 2004. *ALS3* and *ALS8* represent a single locus that encodes a *Candida albicans* adhesin; functional comparisons between Als3p and Als1p. Microbiology **150**:2415–2428.

Zhao X, Oh S-H, Hoyer LL. 2007. Deletion of *ALS5*, *ALS6* or *ALS7* increases adhesion of *Candida albicans* to human vascular endothelial and buccal epithelial cells. Med Mycol. **45**:429–434.

Zhao X, Oh S-H, Yeater KM, Hoyer LL. 2005. Analysis of the *Candida albicans* Als2p and Als4p adhesins suggests the potential for compensatory function within the Als family. Microbiology **151**: 1619–1630.

Communicating editor: A. Mitchell